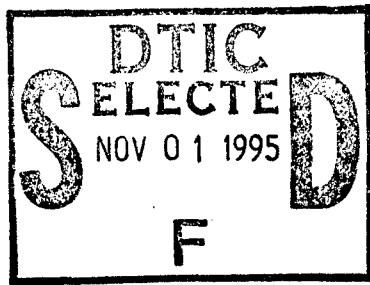


UNCLASSIFIED

AD NUMBER
ADB204323
NEW LIMITATION CHANGE
TO Approved for public release, distribution unlimited
FROM Distribution authorized to DoD only; Specific Authority; Proprietary Info.; 1 Nov 95. Other requests shall be referred to Army Medical Research and Materiel Command, Attn: MCMR-RMI-S, Fort Detrick, MD 21702-5012.
AUTHORITY
USAMRMC ltr dtd 21 Jan 2000

THIS PAGE IS UNCLASSIFIED



AD _____

CONTRACT NUMBER: DAMD17-95-C-5042

TITLE: Development of Non-Invasive Deep Tissue pH Sensor

PRINCIPAL INVESTIGATOR: Dr. Ronald Micheels

CONTRACTING ORGANIZATION: Polestar Technologies Inc
Sudbury, Massachusetts 01776

REPORT DATE: October 1995

TYPE OF REPORT: Final, Phase I

PREPARED FOR: U.S. Army Medical Research and Materiel Command
Fort Detrick, Maryland 21702-5012

PROPRIETARY INFORMATION

DISTRIBUTION STATEMENT: Distribution authorized to DoD Components only, Specific Authority. Other requests shall be referred to the Commander, U.S. Army Medical Research and Materiel Command, ATTN: MCMR-RMI-S, Fort Detrick, MD 21702-5012

The views, opinions and/or findings contained in this report are those of the author(s) and should not be construed as an official Department of the Army position, policy or decision unless so designated by other documentation.

19951030 106

DTIC QUALITY INSPECTED 5

REPORT DOCUMENTATION PAGE

Form Approved
OMB No. 0704-0188

Public reporting burden for this collection of information is estimated to average 1 hour per response, including the time for reviewing instructions, searching existing data sources, gathering and maintaining the data needed, and completing and reviewing the collection of information. Send comments regarding this burden estimate or any other aspect of this collection of information, including suggestions for reducing this burden, to Washington Headquarters Services, Directorate for Information Operations and Reports, 1215 Jefferson Davis Highway, Suite 1204, Arlington, VA 22202-4302, and to the Office of Management and Budget, Paperwork Reduction Project (0704-0188), Washington, DC 20503.

1. AGENCY USE ONLY (Leave blank)	2. REPORT DATE October 1995	3. REPORT TYPE AND DATES COVERED Final, Phase I 15 Mar 95 - 14 Sep 95
4. TITLE AND SUBTITLE Development of Non-Invasive Deep Tissue pH Sensor		5. FUNDING NUMBERS DAMD17-95-C-5042
6. AUTHOR(S) Dr. Ronald Micheels		
7. PERFORMING ORGANIZATION NAME(S) AND ADDRESS(ES) Polestar Technologies Inc. Sudbury, Massachusetts 01776		8. PERFORMING ORGANIZATION REPORT NUMBER
9. SPONSORING/MONITORING AGENCY NAME(S) AND ADDRESS(ES) U.S. Army Medical Research and Materiel Command Fort Detrick, Maryland 21702-5012		10. SPONSORING/MONITORING AGENCY REPORT NUMBER
11. SUPPLEMENTARY NOTES		

PROPRIETARY INFORMATION

12a. DISTRIBUTION/AVAILABILITY STATEMENT Distribution authorized to DoD components only, Specific Authority. Other requests shall be referred to the Commander, U.S. Army Medical Research and Materiel Command, ATTN: MCMR-RMI-S, Fort Detrick, MD 21702-5012	12b. DISTRIBUTION CODE
---	------------------------

13. ABSTRACT (Maximum 200 words)

A Phase I SBIR effort has demonstrated the feasibility of measuring deep tissue pH using near infrared reflection spectroscopy coupled with partial least squares multivariate calibration techniques. Measurement of pH with a breadboard system has been successfully demonstrated in skin covered rabbit muscle and in a canine heart on cardiopulmonary bypass. In six separate determinations of deep tissue pH in the rabbit teres major muscle, the derived model was capable of measuring pH from collected near-infrared spectra to an average accuracy of -0.006 ± 0.009 pH units. By collecting data on both the canine heart and the rabbit muscle, the potential of this technique for diagnosis of ischemic conditions in muscle tissue has been shown.

The Phase I effort has demonstrated the following characteristics for this pH measurement system: significant measurement penetration down to a depth of 7 mm, insensitivity to probe height from skin/muscle surface, and a measurement time of under 15 seconds. The results of the Phase I effort are promising for development of a miniaturized, low cost non-invasive pH monitor system for assisting combat casualties in the field, as well as for many civilian medical applications, including cardiac and reconstructive surgery.

14. SUBJECT TERMS non-invasive near-infrared, reflection sensor tissue pH combat casualties			15. NUMBER OF PAGES 44
			16. PRICE CODE
17. SECURITY CLASSIFICATION OF REPORT Unclassified	18. SECURITY CLASSIFICATION OF THIS PAGE Unclassified	19. SECURITY CLASSIFICATION OF ABSTRACT Unclassified	20. LIMITATION OF ABSTRACT limited

GENERAL INSTRUCTIONS FOR COMPLETING SF 298

The Report Documentation Page (RDP) is used in announcing and cataloging reports. It is important that this information be consistent with the rest of the report, particularly the cover and title page. Instructions for filling in each block of the form follow. It is important to *stay within the lines* to meet optical scanning requirements.

Block 1. Agency Use Only (Leave blank).

Block 2. Report Date. Full publication date including day, month, and year, if available (e.g. 1 Jan 88). Must cite at least the year.

Block 3. Type of Report and Dates Covered. State whether report is interim, final, etc. If applicable, enter inclusive report dates (e.g. 10 Jun 87 - 30 Jun 88).

Block 4. Title and Subtitle. A title is taken from the part of the report that provides the most meaningful and complete information. When a report is prepared in more than one volume, repeat the primary title, add volume number, and include subtitle for the specific volume. On classified documents enter the title classification in parentheses.

Block 5. Funding Numbers. To include contract and grant numbers; may include program element number(s), project number(s), task number(s), and work unit number(s). Use the following labels:

C - Contract	PR - Project
G - Grant	TA - Task
PP - Program Element	WU - Work Unit Accession No.

Block 6. Author(s). Name(s) of person(s) responsible for writing the report, performing the research, or credited with the content of the report. If editor or compiler, this should follow the name(s).

Block 7. Performing Organization Name(s) and Address(es). Self-explanatory.

Block 8. Performing Organization Report Number. Enter the unique alphanumeric report number(s) assigned by the organization performing the report.

Block 9. Sponsoring/Monitoring Agency Name(s) and Address(es). Self-explanatory.

Block 10. Sponsoring/Monitoring Agency Report Number. (If known)

Block 11. Supplementary Notes. Enter information not included elsewhere such as: Prepared in cooperation with...; Trans. of...; To be published in.... When a report is revised, include a statement whether the new report supersedes or supplements the older report.

Block 12a. Distribution/Availability Statement. Denotes public availability or limitations. Cite any availability to the public. Enter additional limitations or special markings in all capitals (e.g. NOFORN, REL, ITAR).

DOD - See DoDD 5230.24, "Distribution Statements on Technical Documents."

DOE - See authorities.

NASA - See Handbook NHB 2200.2.

NTIS - Leave blank.

Block 12b. Distribution Code.

DOD - Leave blank.

DOE - Enter DOE distribution categories from the Standard Distribution for Unclassified Scientific and Technical Reports.

NASA - Leave blank.

NTIS - Leave blank.

Block 13. Abstract. Include a brief (*Maximum 200 words*) factual summary of the most significant information contained in the report.

Block 14. Subject Terms. Keywords or phrases identifying major subjects in the report.

Block 15. Number of Pages. Enter the total number of pages.

Block 16. Price Code. Enter appropriate price code (*NTIS only*).

Blocks 17. - 19. Security Classifications. Self-explanatory. Enter U.S. Security Classification in accordance with U.S. Security Regulations (i.e., UNCLASSIFIED). If form contains classified information, stamp classification on the top and bottom of the page.

Block 20. Limitation of Abstract. This block must be completed to assign a limitation to the abstract. Enter either UL (unlimited) or SAR (same as report). An entry in this block is necessary if the abstract is to be limited. If blank, the abstract is assumed to be unlimited.

FOREWORD

Opinions, interpretations, conclusions and recommendations are those of the author and are not necessarily endorsed by the US Army.

Where copyrighted material is quoted, permission has been obtained to use such material.

Where material from documents designated for limited distribution is quoted, permission has been obtained to use the material.

KWM Citations of commercial organizations and trade names in this report do not constitute an official Department of Army endorsement or approval of the products or services of these organizations.

KWM In conducting research using animals, the investigator(s) adhered to the "Guide for the Care and Use of Laboratory Animals," prepared by the Committee on Care and Use of Laboratory Animals of the Institute of Laboratory Resources, National Research Council (NIH Publication No. 86-23, Revised 1985).

For the protection of human subjects, the investigator(s) adhered to policies of applicable Federal Law 45 CFR 46.

In conducting research utilizing recombinant DNA technology, the investigator(s) adhered to current guidelines promulgated by the National Institutes of Health.

In the conduct of research utilizing recombinant DNA, the investigator(s) adhered to the NIH Guidelines for Research Involving Recombinant DNA Molecules.

In the conduct of research involving hazardous organisms, the investigator(s) adhered to the CDC-NIH Guide for Biosafety in Microbiological and Biomedical Laboratories.

Accession For	
NTIS	CRA&I <input checked="" type="checkbox"/>
DTIC	TAB <input checked="" type="checkbox"/>
Unannounced	<input type="checkbox"/>
Justification	
By	
Distribution/	
Availability Codes	
Dist	Avail and/or Special
E-4	

Ronald H. Mendenhall 9/26/85
PI - Signature Date

TABLE OF CONTENTS

	PAGE
1.0 INTRODUCTION	1
1.1 Problem Description and Background	2
1.2 Approach	2
2.0 DEFINITION OF PROGRAM REQUIREMENTS	5
3.0 EXPERIMENTAL METHODS	5
3.1 Surgical Methods	5
3.2 Microelectrode pH Measurement	6
3.3 Near-infrared Spectrometer and Probe Systems	7
3.4 Partial Least Squares Analysis	11
3.5 Experiments with Myoglobin in pH Buffer Solutions as a Model Compound for NIR Spectral Determination of pH in Muscle Tissue	12
3.6 Experiments to Determine the Depth Penetration of the NIR Reflection Technique for Tissue pH	12
3.7 Data Analysis	12
4.0 RESULTS	12
4.1 pH Electrode Measurements	12
4.2 Rabbit Experiments	15
4.3 Dog Experiments	20
4.4 Myoglobin as a Model Compound for the NIR Spectral Determination of pH in Muscle Tissue	23
4.5 Analysis of NIR Spectra and pH Data to Determine Minimum Required Spectral Resolution Elements	23
4.6 Experiments to Determine the Depth Penetration of the NIR Reflection Technique for Tissue pH Measurement	28
5.0 DISCUSSION	28

	PAGE
6.0 CONCEPTUAL DESIGN FOR PROTOTYPE MINIATURE NEAR-INFRARED DEEP TISSUE pH MONITOR	31
7.0 RECOMMENDATIONS FOR CONTINUED WORK	33
8.0 CONCLUSIONS	33
9.0 REFERENCES	35

Accession For		
NTIS	CRA&I	<input type="checkbox"/>
DTIC	TAB	<input type="checkbox"/>
Unannounced		<input type="checkbox"/>
Justification		
By		
Distribution /		
Availability Codes		
Dist	Avail and/or Special	

LIST OF FIGURES

		PAGE
Figure 1.	Diagram of Near-Infrared Fiber-optic Spectroscopy System for Non-Contact pH Measurement in Human or Animal Tissue	8
Figure 2.	Fiber-optic Reflectance Probe Configurations Used for NIR pH Measurement: (a) collinear, bifurcated probe; (b) 60° angled probe	9
Figure 3.	Photographs of Experimental Set-up Used for NIR pH Measurements in Rabbit Subjects	10
Figure 4.	Continuous Micro-electrode pH Traces for Electrodes 1 and 2 for Rabbit 11J for Muscle Covered with Skin	14
Figure 5.	Continuous Micro-electrode pH Traces for Electrodes 1 and 2 in Dog 28I, Right Heart Ventricle Wall	16
Figure 6.	NIR Reflection Spectra of Rabbit Muscle Flap Covered with Skin, Measured with the NIR Systems Spectrometer	17
Figure 7.	Partial Least Squares Calibration Verification Plot of Actual vs. Predicted pH (from NIR spectra) for Rabbit 11J	18
Figure 8.	Partial Least Squares Calibration Verification Plot of Actual vs. Predicted pH (from NIR spectra) for Dog 28I	22
Figure 9.	Transmission Spectra for 23 Myoglobin Samples in Different pH Buffers	24
Figure 10.	Partial Least Squares Calibration Plot of Actual vs. Predicted pH (from NIR spectra) for Myoglobin Dissolved in pH Buffer Solutions	25
Figure 11.	NIR Reflection Spectrum of Rabbit Muscle Tissue with Normal Resolution of 201 Wavelength Points in 700-1100 nm Range	26

	PAGE
Figure 12. Partial Least Squares Calibration Verification Plot of Actual vs. Predicted pH (from NIR spectra) for Rabbit 13J	27
Figure 13. NIR Reflection Spectra of a 7 mm Flank Steak Sample,	29
Figure 14. Conceptual Design for Compact Deep Tissue pH Sensor	32

LIST OF TABLES

	PAGE
Table I. pH Data Collected from Rabbit Experiments	13
Table II. Model Statistics Derived from Rabbit Experiments	19
Table III. Comparison of Model Statistics for Two Different Wavelength Regions	21
Table IV. Predicted pH for Deep Muscle Tissue Covered with a Skin Flap: 700-1100 nm	21
Table V. Model Statistics Derived from Canine Experiments	21

1.0 INTRODUCTION

Polestar Technologies, Inc. has completed for the U. S. Army Medical Research and Material Command under Contract No. DAMD17-95-C-5042 a Phase I SBIR effort entitled "Development of Non-Invasive Deep Tissue pH Sensor." This program was to develop a non-invasive sensor and monitor system utilizing the intrinsic optical properties of pigments present in muscle and organ tissue to detect tissue pH. This system will provide additional critical information to medical personnel making triage decisions on the battlefield. Because of its small size and portability, it will be easily incorporated into evacuation helicopters and ambulances as well as hospital operating rooms, intensive care units, and body-worn monitor systems. The Phase I objectives were to demonstrate the feasibility of the approach through the primary tasks summarized below:

Task 1	System requirements definition
Task 2	Sensor/system design and construction for Phase I experiments
Task 3	Experimental verification of proposed measurement technique
Task 4	Final system conceptual design

Success has been realized in each of these areas. System specifications which would support the Army's requirements were defined and included sensor range of measurement, accuracy, and response time as well as physical size and computer interface requirements. Fiber optic probes were designed and constructed to interface with both a portable spectrometer and a near-infrared spectrometer. Experiments were conducted on fourteen subjects and proved that the prototype monitor system successfully demonstrated performance characteristics as stated below:

- a pH accuracy of 0.01 pH units in muscle tissue covered with skin
- significant measurement penetration down to a depth of 7 mm
- insensitivity to probe height from skin/muscle surface
- a measurement time of 15 seconds
- a partial least squares calibration model with a reproducible R^2 coefficient better than 0.98 and route mean square deviation errors less than 0.02 pH units

A conceptual design for a dedicated portable near-infrared pH monitor system for diagnosis of combat casualties in the battlefield has been developed.

The accomplishments of this Phase I program indicate a high probability of success in future development efforts to develop a fieldable non-invasive pH sensor for critical care diagnostic applications, both on the battlefield and in civilian environments. Additionally, other applications such as cardiac, reconstructive, and abdominal surgery, to suggest a few, would clearly benefit from the commercialization of this technology.

1.1 Problem Description and Background

The US Army is interested in equipping its soldiers with small body-worn sensors to continuously measure deep tissue pH. Tissue pH is an excellent indicator of cell metabolic state. As oxygen delivery to cells is reduced, the cells are still able to hydrolyze adenosine triphosphate (ATP) to produce energy through anaerobic metabolism; the by-products of this process are hydrogen ions and lactic acid. Ischemia is accompanied by reduced blood flow; and, under this condition, both the lactic acid and hydrogen ions accumulate resulting in a decrease in the pH of both the cell and the interstitial fluid surrounding the cell. The measurement of tissue pH with implanted electrodes measures the interstitial pH. Implanted sensors have been successfully used to monitor changes in tissue pH during hemorrhagic shock (1), free-flap transfer during reconstructive surgery (2,3), and during cardioplegic arrest during open heart surgery (4,5). However, implantable sensors are impractical for continuous monitoring on healthy individuals; and a non-invasive sensor is required.

Nuclear magnetic resonance (NMR) has been used in the laboratory to measure intracellular pH. This technique does not easily extend itself to miniaturization. Doppler ultrasound has been used as a non-invasive measurement of blood flow; however, this technique provides poor directional information and lacks the physiological information about oxygen delivery that the tissue pH measurement provides. The ability to non-invasively measure tissue oxygenation using near-infrared spectroscopy has been reported by Hampson and Piantadosi (6) and Wilson et. al. (7). By measuring explicit single wavelength changes in the absorption spectra of hemoglobin, myoglobin, and cytochrome aa_3 , these authors have demonstrated changes in tissue oxygenation due to ischemia; however, changes in tissue oxygenation do not tell the entire story. During tourniquet ischemia in a human forearm, muscle oxygen stores are depleted in six minutes (6). Measurements show that tissue pH reaches a minimum after 60-90 minutes of ischemia, indicating that anaerobic metabolism is active during that time (3). Tissue pH measurement is an important adjunct in assessing the status of an injured soldier on the battlefield and during transit to a field hospital.

Currently, there is no known method of non-invasively measuring tissue pH with a miniature device. This report describes the first known in-vivo demonstration of a non-invasive measurement of tissue pH using near-infrared spectroscopy.

1.2 Approach

This non-invasive deep tissue pH monitor takes advantage of the intrinsic optical properties of the pigments present in muscle cells. These pigments absorb light in the near-infrared spectrum, and include hemoglobins, myoglobins, cytochromes, flavoproteins, pyridine nucleotides, and melanin. As with any organic or biological molecule, the absorption properties are dependent on the nature of the matrix surrounding that molecule. In particular, pH of the "solution" surrounding the molecules will affect the absorbance properties of the molecule. It is this variation in absorbance properties with pH that is the basis of the monitor. As the pH of interstitial fluid changes as a result of the accumulation of hydrogen ions during ischemia, the absorption spectrum of the pigments in

the muscle cells will also change. By monitoring these subtle changes in the absorption spectrum of muscle tissue, we can determine the pH of the fluid surrounding the cells, i.e., the tissue pH. There is a recent report (8) in which near-infrared transmission spectra were recorded for a number of model compounds including amines, peptides and proteins in aqueous solutions at two widely separated pH levels (pH 2 and 8). The results of this study showed significant changes in the NIR spectra of these compounds, associated with pH changes, but these changes were not quantified with any type of calibration model. Another recent article (9) reports measurement of pH from NIR transmission spectra in saline solutions of glucose and human serum albumin where a calibration model is developed, but the wavelength region utilized, 1130 - 1980 nm, is not useful for deep muscle tissue measurements because of shallow penetration depths and water interference associated with this range. Also, the pH predicted error for this latter study was large (0.3 pH units).

Near-infrared (NIR) spectroscopy, coupled with multivariate calibration techniques, has been widely used in the determination of protein and fat in meat products (10 - 12). It is just starting to gain acceptance as a technique to non-invasively determine chemical concentrations in blood and tissue. Near-infrared light in the wavelength region of 700-2500 nm is known to penetrate through the skin and bones without being absorbed, allowing for the measurement of blood and tissue components (13). Making use of the complex optical spectra collected from living tissue requires the application of recently available tools from the field of chemometrics. Multivariate calibration techniques, including partial least squares (PLS) and principal component regression (PCR) analysis, are employed to derive calibration models which relate multiwavelength spectral data to an independent determination of the concentration of the analyte of interest.

There have been many reports, over the last ten years, on the use of near-infrared (NIR) reflectance and transmission spectroscopy as a non-contact method to measure protein, fat, and water in meat products with high accuracy (10 - 12). These NIR-based characterization methods for meat have utilized the 800 - 1,850 nm region of the spectrum (10). NIR transmission measurements in the 800 - 1,100 nm wavelength region were reported for 15 mm thick beef samples (10). A transmission pathlength of 15 mm in beef would indicate that a reflection measurement which involves a double pass through the sample thickness could probe down to a depth about one half of this distance or about 7.5 mm. Results of this study, presented in Section 4.0, confirmed that the features of the NIR spectra of meat samples are very similar to that of living muscle tissue..

One of the most widely known biomedical applications of near-infrared spectroscopy and multivariate calibration methods is the non-invasive measurement of blood glucose in diabetic patients. In a series of articles Haaland et. al. (14 - 16) demonstrated the application of PLS and PCR techniques to measure glucose in whole blood removed from patients and as an in-vivo determination. While there are still many details to work out before this technique can be widely used, they demonstrated a prediction error of 1-2 mmol/L on human subjects monitored through the finger (16).

Recently Carney et. al. (17) used near-infrared monitoring to analyze changes in lipids and proteins present in gerbil brains which have undergone strokes. Using a commercial spectrometer and their own multivariate calibration techniques (BEAST), they measured these changes in frozen brain samples as well as in live gerbils which had undergone strokes.

In cases of chemical systems consisting of a complex mixture of many components which exhibit very broad spectral features, a set of statistical analysis methods referred to as multivariate calibration or regression analysis has been successfully used for the last twelve years to develop a calibration relation between spectroscopic data and known concentrations of a set of calibration samples (1, 10 - 12, 18, 19). This multivariate calibration technique has been particularly successful for analysis of near-infrared spectra of biological samples such as protein and fat in meat and glucose in blood. Partial least squares (PLS) regression analysis is one of the most commonly used types of multivariate calibration analysis and has been employed in this Phase I development effort.

The basic theory of PLS regression analysis of the relation between a set of absorbance vs. wavelength spectra and the corresponding known concentrations of a chemical component, which is the muscle tissue pH in this case, can be described (12, 18, 19) by the following equation:

$$pH_i = \sum_{k=1}^K (A_{ik} \cdot R_{ik})$$

where pH_i is the pH of sample i in a calibration set, the index k is for the wavelengths measured in the NIR spectra (k is the total number of wavelengths points), R_{ik} is the spectral reflectance (in $\log(1/\text{reflectance})$ units) for sample i at wavelength k , and A_{ik} are the PLS regression coefficients which must be calculated by the regression analysis. PLS software packages are currently available as commercial products from a number of suppliers. To determine a calibration model relating spectral data to pH values, a calibration set of NIR spectra together with corresponding known pH values are entered into the PLS analysis program which determines the optimal regression coefficients along with other statistical information regarding the quality and accuracy of the calibration model.

Reflected near-infrared light can be easily measured from anywhere on the body and processed remotely to determine pH. This technique not only has the potential to provide miniature, body-worn sensors for soldiers in the battlefield, but can be adapted for civilian uses. Similar sensors can be worn by patients who have undergone reconstructive surgery to assess adequacy of arterial and venous connections for twenty-four hours after surgery. Hand-held devices might be used to assess the adequacy of myocardial protection and vein graft perfusion during open heart surgery. Other hand-held devices could be used by emergency personnel to monitor shock in civilian trauma victims. The work in this Phase I effort consisted of a series of experiments with rabbit and dog subjects which demonstrates the feasibility of non-invasive near-infrared monitoring of tissue pH.

2.0 DEFINITION OF PROGRAM REQUIREMENTS

The requirements of the Army for a non-invasive deep tissue pH monitor to be used in combat casualty diagnostic applications were discussed in detail with the program technical contract monitor. For the Phase I program, the ideal desired technical specifications for the pH monitor were a pH resolution of 0.1 - 0.05 pH units, a depth penetration of 1 cm, a response time no longer than 15 sec, and the potential for configuration of the measurement system in a miniaturized and low cost portable package that could be worn on the body of a soldier at single or multiple sites. The primary diagnostic function for the system is described as a means of determining if a combat casualty is in a state of shock from hemorrhaging, the severity of hemorrhaging as well as the time available for corrective action.

3.0 EXPERIMENTAL METHODS

3.1 Surgical Methods

Surgery was performed on fourteen rabbits in the Phase I study. The rabbits were preanesthetized with a ketamine/xylazine mixture, and their abdomens and backs were shaved and cleaned. A tracheal tube was placed, and the animal ventilated with approximately 2% isoflurane plus 98% oxygen (tidal volume \approx 90 ml, rate \approx 30 breaths/min). The carotid artery was dissected, and a Millar pressure transducer placed to monitor systemic blood pressure. The femoral artery was exposed, and a 20 Gauge catheter was placed to facilitate the collection of blood samples for blood gas analysis. The blood gas samples were used to adjust ventilation during the experiment to maintain proper acid-base balance. First, the right latissimus dorsi muscle flap was removed to expose the teres major muscle on the right side. The teres major muscle was dissected from the scapula, and the single artery feeding the muscle was isolated. The muscle was stitched flat on top of a chemical heating pad. Electrochemical pH probes 1.3 mm in diameter were implanted along the left and right sides of the teres major muscle. The agar bridge, which connects the implanted electrodes to the reference electrode, was implanted in fat under the skin, against the rabbit's back muscle. A temperature probe was implanted with at least one of the pH probes. A vascular clamp was placed across the artery connecting the teres major muscle to the rest of the rabbit. In experiments where spectra were measured through skin a piece of skin approximately 1 inch by 2 inches was cut from the rabbit from the area which was over the latissimus dorsi muscle. The skin was shaved of fur, and the fascia was removed. The skin was placed fur side down on top of the bare muscle to be measured. Once the spectrometer probe was aligned, the clamp was closed to initiate ischemia. pH was monitored continually; and when the pH no longer decreased, usually after 60-90 minutes, the clamp was opened to begin reperfusion of the teres major muscle. On occasion the experiment was repeated on the left side of the rabbit as well. The animals were humanely euthanized at the completion of the experiment.

pH and spectroscopic data were also collected from two dogs which were undergoing cardiac surgery procedures for a separate experiment. Dogs were preanesthetized with acepromazine and sodium pentothal. After tracheal intubation the dogs were ventilated with 1-2% halothane mixed

with oxygen. EKG electrodes were placed to monitor heart rate, and a Millar pressure transducer was placed in the right femoral artery catheter to monitor systemic blood pressure. Following median sternotomy and opening of the pericardium, two pH probes were placed in the right ventricle wall. The left femoral artery was dissected, and the arterial cannula placed. A 14-gauge catheter was then placed in the aortic root for delivery of cardioplegia solution. A two-stage venous cannula was inserted in the superior and inferior vena cavae, and the animal was placed on cardiopulmonary bypass. After a stable blood pressure was established, the aorta was cross-clamped to initiate global ischemia. After 10 minutes of ischemia a blood-based cardioplegia solution (pH 7.6) was administered for 30 minutes. pH and spectroscopic data were collected for the ischemia and cardioplegia reperfusion periods.

All animals received humane care in compliance with the "Principles of Laboratory Animal Care" formulated by the National Society for Medical Research and the "Guide for the Care and Use of Laboratory Animals" prepared by the National Academy and published by the National Institutes of Health (NIH Publication No 85-23, revised, 1985).

3.2 Microelectrode pH Measurement

Microelectrode pH measurement is performed using methods described by Khuri (20). Briefly small glass electrodes are implanted to a depth of approximately 5 mm in the muscle tissue to be measured. The microelectrode is attached to a larger reference electrode (outside the subject) through an agar bridge implanted in fat elsewhere in the animal's body. Thermistor probes are placed adjacent to the pH probes to measure temperature. The data was collected on a custom system built in the University of Massachusetts Medical Center laboratories. The system was designed to use 1.3 mm Esophageal pH Electrodes (model MI-506, Microelectrodes, Inc., Bedford, NH) with a needle reference electrode/agar bridge set (models 10112, 100790, Vascular Technologies, Inc., Chelmsford, MA) and thermistor temperature probes (model 2123, Medtronics, Inc.)

The pH probes and reference electrodes were connected through a high impedance converter to the data acquisition board (AT-MIO-64F-5, National Instruments), configured in the differential input mode. The board is installed in a NEC PowerMate VP75 personal computer and programmed with National Instruments NI-DAQ control library using LabVIEW graphical programming language.

Data acquisition for the calibration routine was accomplished by sampling the channels at 2500 Hz and averaging over one second. Calibration of an individual channel is deemed complete when 300 consecutive data points (5 minutes data collection) are all within $\pm 1\%$ of the average of the data set. The calibration procedure records voltage measurements at pH 6.0 and pH 7.4 values and computes the linear relationship between voltage and pH for each electrode. The data acquisition routine acquires data at 2500 Hz and averages for 10 seconds. pH is calculated from the calibration equations and is continually displayed in digital and graphical form. The pH data is written to disk every 15 minutes.

Temperature correction routines are available to correct the electrode response to temperature, but were not needed for data collected above 30°C.

3.3 Near-infrared Spectrometer and Probe Systems

In the Phase I work, two different NIR spectrometers and fiber-optic reflection probe designs were used. Data from experiments R1J-R6J and experiment R8J were collected on an Ocean Optics (Dunedin, FL) spectrometer in the wavelength region from 500-1000 nm. The Ocean Optics system is based on a fixed angle diffraction grating spectrometer with 1024 element Si CCD array detector and has a spectral resolution of about 3 nm. This spectrometer is very compact and is powered by, and interfaced to, a notebook computer, making the complete system very portable with a total weight of less than 10 lbs. Data from the remaining rabbit experiments, as well as the two dog experiments were collected in the wavelength range 400-2500 nm on a model 6500 spectrometer from NIRSystems Inc. (Silver Spring, MD). The spectral resolution was 10 nm with spectral collection at 2 nm intervals. Thirty-two co-added scans were obtained for each sample on the rabbit, and 16 scans on the dog. Reflection from aluminum foil was used as the reference spectrum for calculating absorbance. Acquisition of a single scan takes 0.9 sec and results in only a 15 sec collection time for the dog heart experiments. The instrument uses a single silicon detector in the 400 - 1100 nm region, a lead sulfide detector in the 1100 - 2500 nm region, and scans spectra with a rapidly rotating diffraction grating.

Fiber optic probes were designed and constructed for use with both spectrometers. The probe was aligned between the two pH probes in the rabbit muscle or dog heart. For each probe configuration the optimal probe height was determined by measuring the intensity of light returned from a reflector, aluminum foil, placed on the rabbit muscle or dog heart. The optimal height was that which gave the largest signal on the spectrometer without saturating the detector. Both an angled 60° and a collinear, bifurcated fiber-optic reflectance probe were used with the Ocean Optics Spectrometer. The generalized overall NIR spectrometer/probe setup is shown in Figure 1. The two probe geometries are shown in Figure 2. An angled 60° probe was used exclusively with the Near-infrared Systems spectrometer. A photograph of the angled probe and 3 axis positioning mount for the Near-infrared Systems spectrometer is given in Figure 3. This figure also shows the most important part of the experimental setup in a rabbit experiment which includes the dissected muscle flap, ligating clamp, pH micro-electrode, temperature sensor, and the NIR probe.

The signal/noise ratio in the reflectance spectra and the accuracy and precision of the pH measurements were superior with the NIR Systems spectrometer because it utilized a much larger diameter fiber probe, light source, and detector, and had a detector/amplifier system with higher stability. The collinear or bifurcated probe geometry results in significantly higher signal throughput and allows probe placement closer to the sample surface than the angled probe.

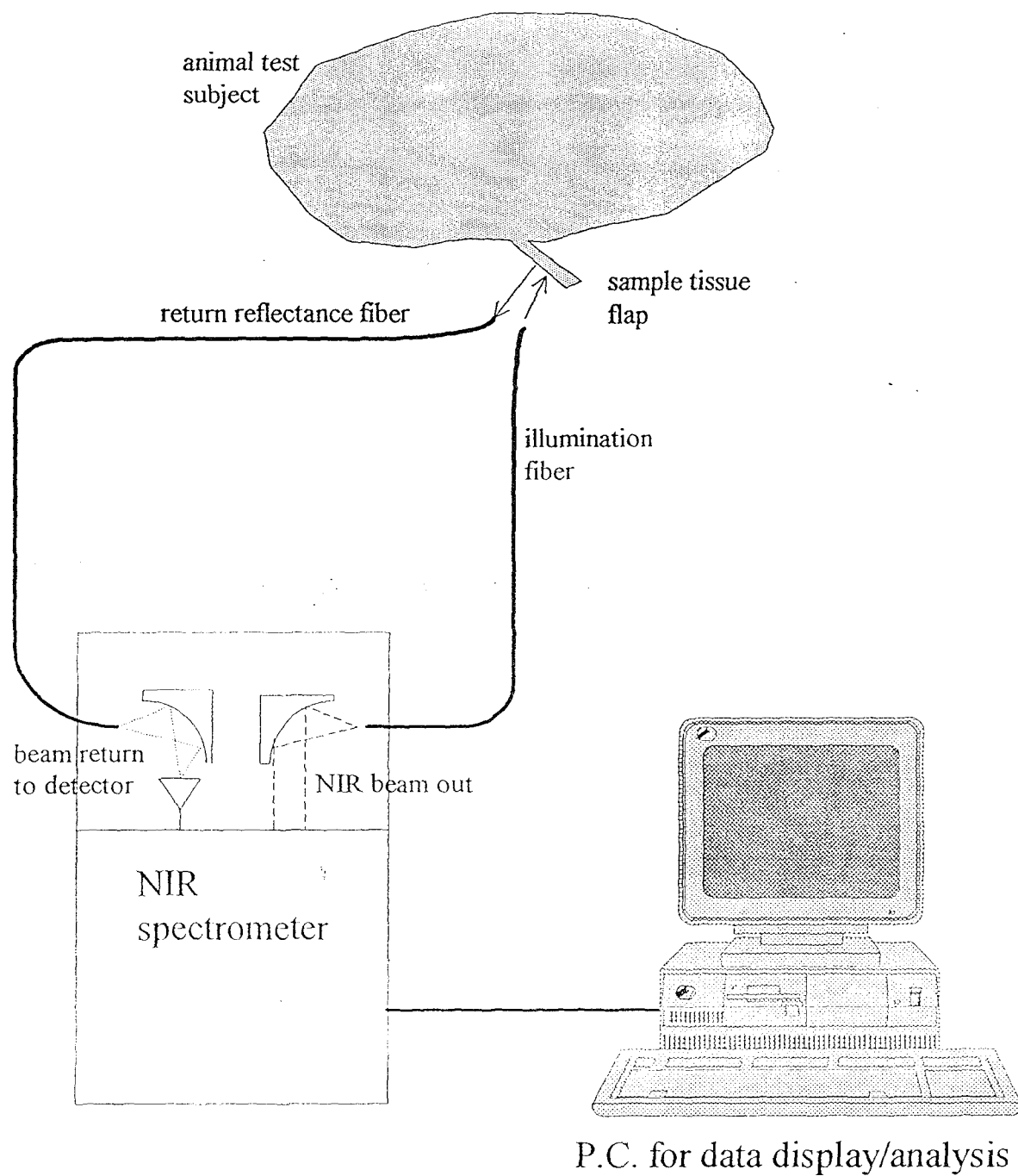


Figure 1. Diagram of near-infrared fiber-optic spectroscopy system for non-contact pH measurement in human or animal tissue

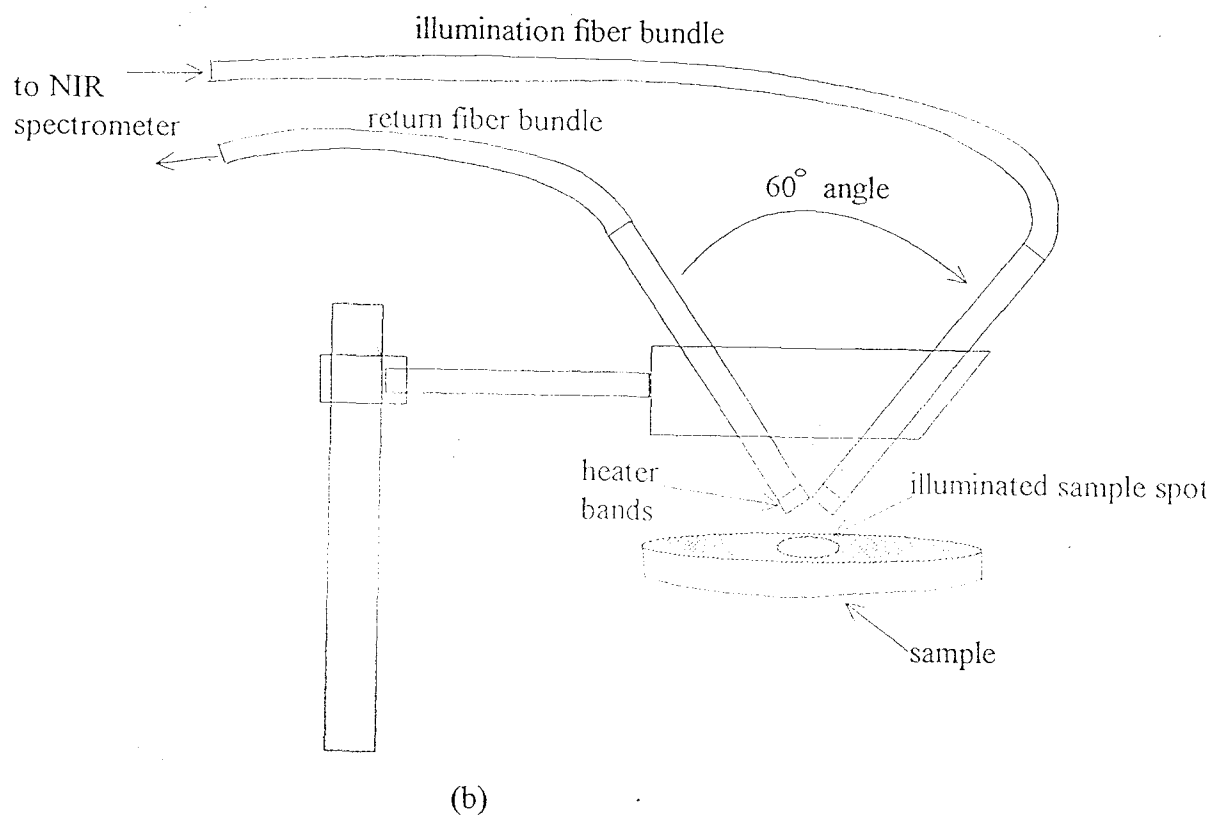
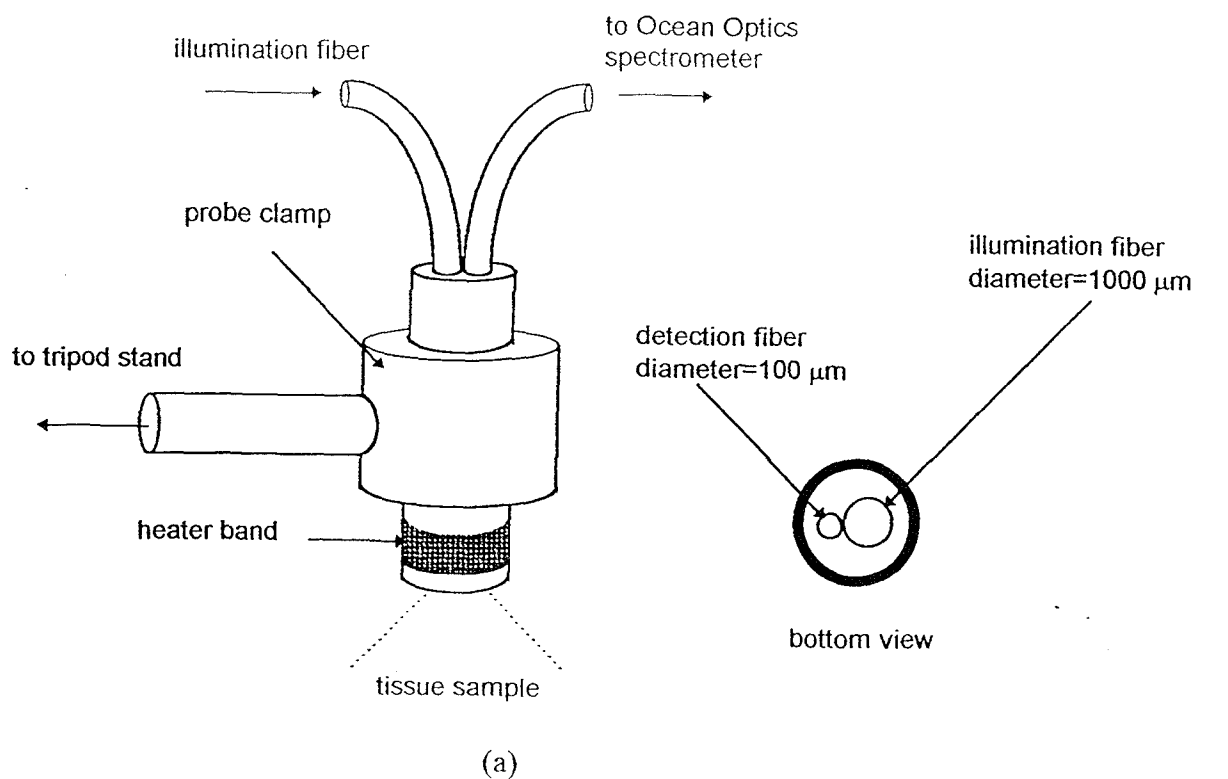
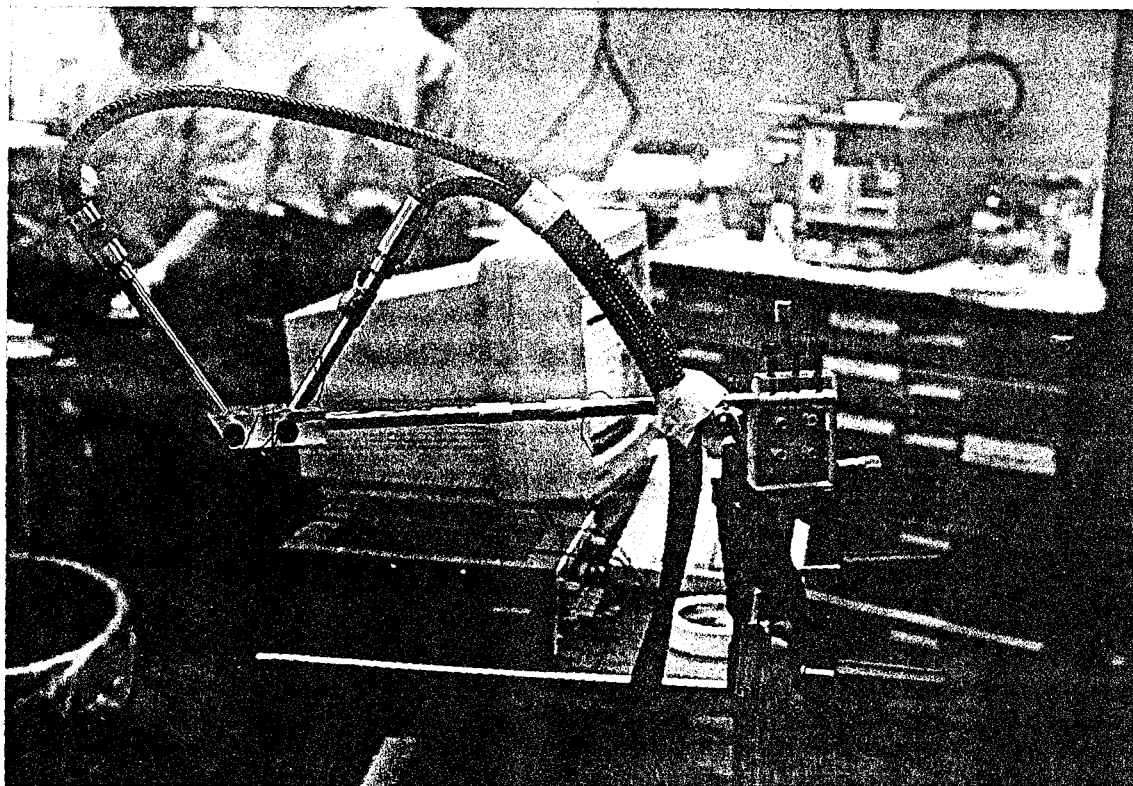


Figure 2. Fiber-optic reflectance probe configurations used for NIR pH measurement: (a) collinear, bifurcated probe, (b) 60° angled probe

a)



b)

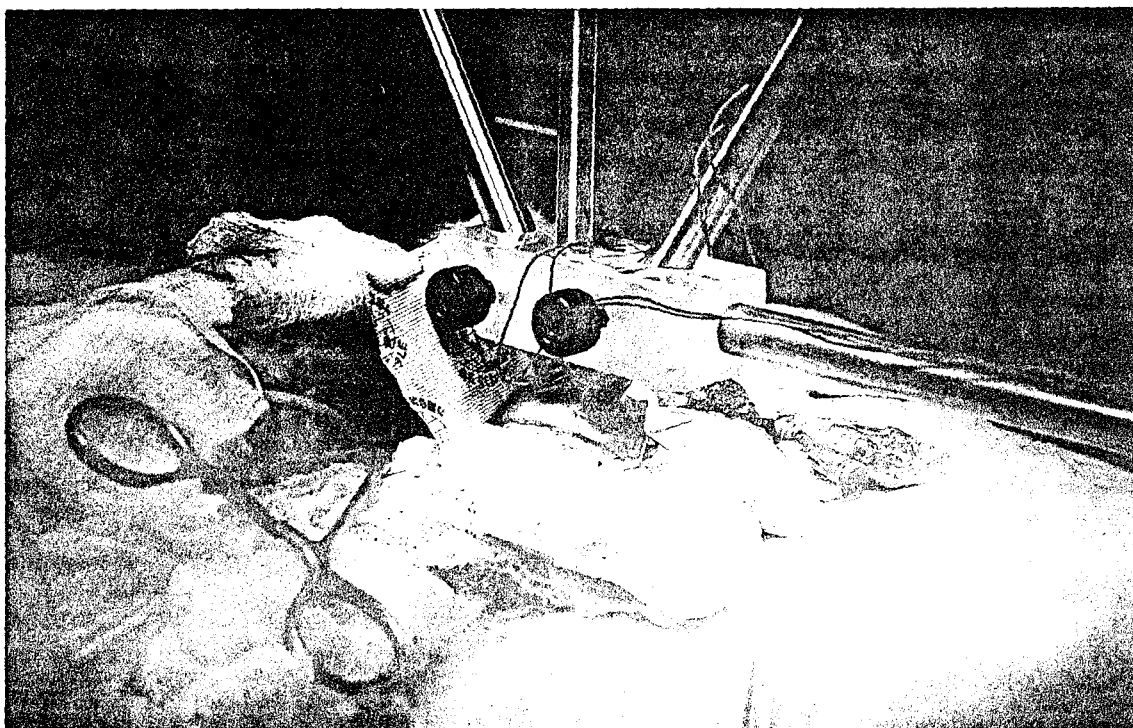


Figure 3. Photographs of experimental setup used for NIR pH measurements in rabbit subjects with NIR Systems spectrometer: (a) 60° angled fiber-optic reflectance probe assembly with x-y-z positioner and angled mount, (b) close-up of angled reflectance probe positioned over muscle flap covered with skin flap, pH microelectrode wire (heavy white wire), and clamp on artery

3.4 Partial Least Squares Analysis

All data processing and model formulation were carried out with Grams/386 software (Galactic Industries Corp.). Data from the Ocean Optics system required significant preprocessing. The reflected light spectra from the sample and the reference were exported as ASCII files to the Grams/386 software where the corresponding absorbance spectra were calculated. The absorbance data were then smoothed with a 21-point Savitsky-Golay smoothing routine. The smoothing removed the high frequency noise components, but did not remove the lower frequency components that were particularly evident between 900-1000 nm. The internal software of the NIRSystems Spectrometer calculated absorbance and smoothed the result. The smoothed absorbance spectra were imported into the Grams/386 software in J-CAMP format.

Using the absorbance data and the recorded pH values from the electrodes, the Partial Least Squares-1 (PLS-1) routine in Grams/386 was used to derive models to predict pH from the corresponding absorbance spectra. Mean-centering was used to process the data before running the PLS-1 routine (21). The PLS-1 routine includes cross-validation to provide many diagnostic features with which to evaluate and fine-tune the model. After the routine is run, the optimal number of regression factors is selected for the model. Grams/386 provides F-ratios and probability values for each factor. The number of factors having a probability value just under 0.75 are selected. Using the optimal number of factors, the actual versus predicted pH is plotted for the model. The derived model is used to predict the pH from each of the sample spectra used to generate the model and the predicted pH is plotted against the actual pH determined with the electrode at that time point. The R^2 value for the plot is a measure of the goodness of the model for predicting pH from the spectral data. A perfect model will have an R^2 value of 1. The root mean squared difference (RMSD) is also reported, and is a measure of the average difference between the actual pH and the value predicted by the model. This metric is a measure of the accuracy of the model in predicting pH, an RMSD of less than 0.1 is considered acceptable for this feasibility study.

The Grams/386 PLS-1 report also provides statistics to identify spectra or concentration values which are outliers. Outliers are those samples that have a spectral or concentration residual F ratio greater than 3 (22) and a probability of being an outlier of greater than 95%. To compare results from individual experiments a model is calculated using the entire wavelength range where absorbance values are less than 3.0, and outliers are identified. The outliers are eliminated, and the model is run once more. The success of the experiment is evaluated from the value of R^2 and RMSD values for each of the rabbits.

Once a model is calculated, it can be used to predict pH values from acquired spectra. For Rabbits 10J - 14J additional models were derived from the remaining 90% of the data points after 10% of the collected spectra were randomly removed to test the model. The model was used to measure pH from the spectra; and the average bias, or difference between actual and predicted pH, was calculated for the set of points.

3.5 Experiments with Myoglobin in pH Buffer Solutions as a Model Compound for NIR Spectral Determination of pH in Muscle Tissue

Solutions with a concentration of 0.25 mg/ml of myoglobin were prepared in 11 different pH buffer solutions which spanned the pH range of 6.3 - 7.3 pH units in 0.1 unit increments. Each solution was prepared at least twice, and a NIR transmission spectra measured for a total of 23 samples. The NIR transmission spectra were measured with the NIR Systems spectrometer using the fiber bundle probes mounted in-line in a metal fixture. The myoglobin spectra were measured with the samples contained in 1 cm pathlength plastic cuvettes. For each sample a separate reference spectrum was measured with the appropriate buffer solution in a 1 cm cuvette without any myoglobin.

3.6 Experiments to Determine the Depth Penetration of the NIR Reflection Technique for Tissue pH

Samples of flank steak obtained from a supermarket were used in these experiments to closely simulate the reflection and transmission characteristics of live rabbit muscle tissue. To determine the penetration depth of the NIR reflection spectroscopy measurements, a special fixture was constructed which supports a small 1" x 1.5" piece of flank steak on a plastic platform with a 0.5" x .75" in rectangular hole in the center to permit the NIR light from the spectrometer fiber-optic reflection probe to pass through. This rectangular hole is spanned by two strands of thread to support the center of the meat sample. A front surface aluminum mirror is held in a slot about 1 mm below the bottom surface of the steak sample so that it can be slid in and out underneath the steak sample without touching it. When present behind the steak sample, the mirror will return an additional reflected NIR component to the receiving fiber bundle of the reflectance probe for any NIR light that passes all the way through the steak sample.

3.7 Data Analysis

All summary data is presented as mean \pm one standard deviation. Statistical analysis was performed on a personal computer using Systat for Windows 5.0.

4.0 RESULTS

4.1 pH Electrode Measurements

pH data from all the rabbit experiments is summarized in Table I. An example of a typical pH versus time trace is shown in Figure 4. Data was typically recorded from two pH electrodes, one of which frequently exhibited a smaller change in pH than the other. For all the rabbit experiments the pH started at a mean value of 7.10 ± 0.25 pH units and dropped to 6.73 ± 0.23 pH units as a result of ligating the artery, for a mean change in pH of 0.37 ± 0.18 . On reperfusion the pH increased from 6.76 ± 0.18 pH units to 7.12 ± 0.29 pH units, a mean change of 0.36 ± 0.22 . Examination of

Table I. pH Data Collected from Rabbit Experiments

experiment number	avg temp	pH1 ligate pH start	pH1 ligate pH end	pH1 reperfuse pH start	pH1 reperfuse pH end	pH2 ligate pH start	pH2 ligate pH end	pH2 reperfuse pH start	pH2 reperfuse pH end
R1J right	27.4	6.80	6.53			6.69	6.35		
R1J left	28.9	6.93	6.35			6.95	6.71		
R2J right	32.6	7.17	6.50			6.81	6.27		
R3J right	28.8	7.12	6.76			7.41	6.94		
R3J left	31.6	6.86	6.52			6.67	6.34		
R4J right	34.3	7.12	6.65	6.65	7.04	7.14	6.63	6.63	7.17
R4J, right, skin	29.8	7.12	6.91			7.43	6.95		
R5J right	31.3	7.35	7.03	6.85	7.36	7.33	6.76	6.69	7.49
R6J right	32.3	6.83	6.69	6.69	6.61	6.77	6.65	6.65	6.60
R6J left	31.2	7.23	7.03	6.99	7.14	7.31	7.11	7.10	7.45
R7J right	35.1	7.17	6.75	6.72	7.46	7.25	7.14	7.12	7.44
R8J left	35.1	7.04	6.55	6.55	7.06	7.02	6.83	6.83	7.04
R9J right	33.4	7.64	7.00	6.98	7.64	7.14	6.75	6.77	7.08
R9J, right, skin	35.7	7.64	7.13			7.20	6.94		
R10J right	37.9	7.20	6.65	6.67	7.22	7.03	6.73	6.74	6.88
R10J right, skin	32.5	7.22	6.99	6.94	7.25	6.95	6.82	6.72	6.89
R11 J right, skin	33.9	7.41	6.53	6.58	7.03	6.94	6.50	6.53	6.62
R12J right, skin	34.0	6.85	6.63	6.66	7.01	7.24	7.02	7.06	7.35
R13J right, skin	31.7	7.35	6.77	6.78	7.23				
R14J right, skin	29.3	6.95	6.74	6.75	7.18				
R14J left, skin	35.4	6.75	6.46	6.42	6.75				

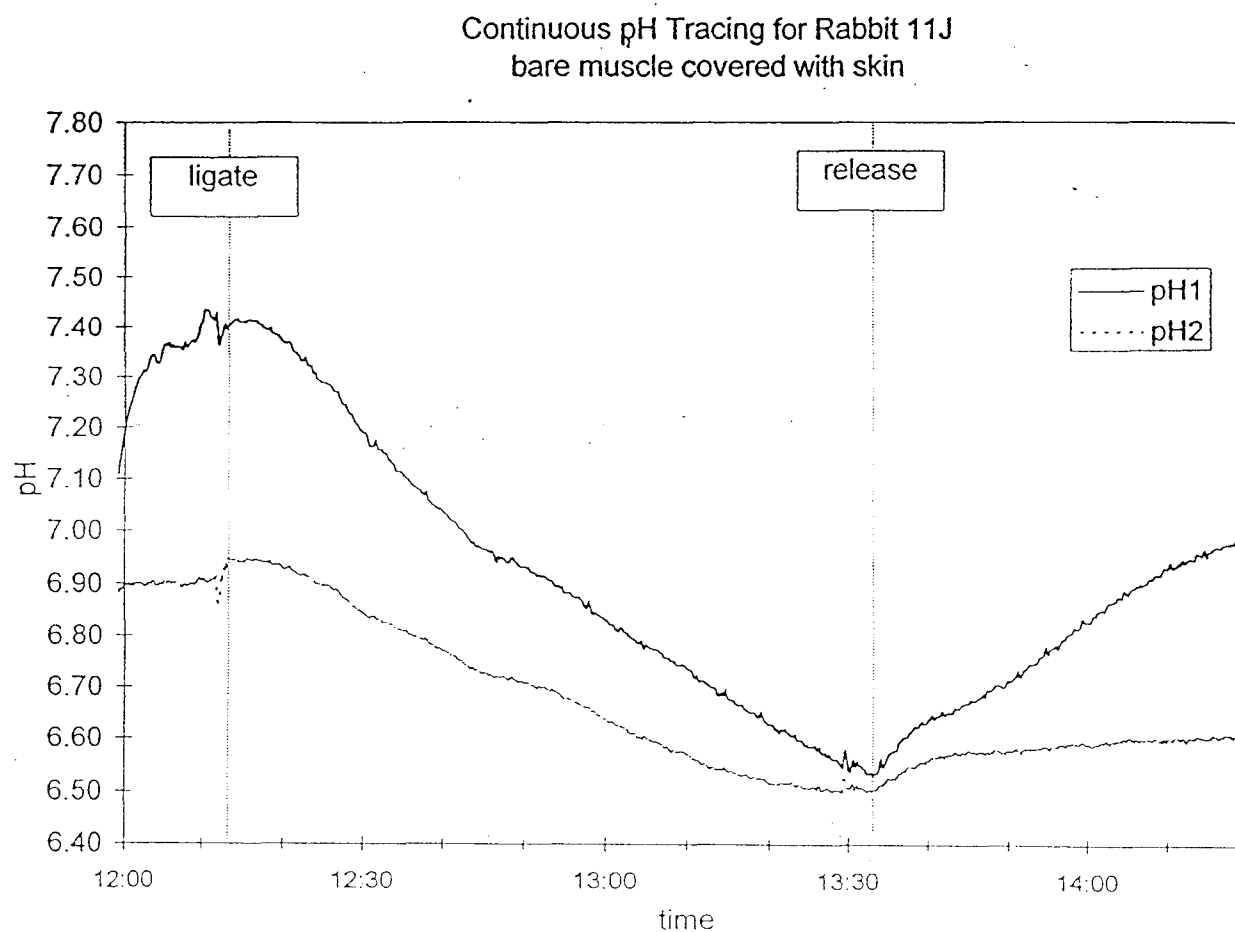


Figure 4. Continuous microelectrode pH traces for electrodes 1 and 2 for Rabbit 11J for muscle covered with skin

individual experiments in Table I shows that in many of the experiments pH change was greater than 0.50 pH units during either ligation or reperfusion, and this change in pH is reflected in the model derived from the data.

In the first few experiments nothing was done to prevent the drop in muscle temperature that occurs as the artery is ligated. This resulted in temperatures below 30°C and a very slow decline in pH during ischemia. In later experiments the addition of a chemical heating pad under the muscle allowed temperatures greater than 31°C to be maintained on almost every experiment resulting in a pH decline of approximately 0.01 pH units/minute. With the chemical heating pad, the temperature change during an experiment was typically less than $\pm 2^\circ\text{C}$.

pH data was collected from two dogs. For Dog27I the baseline pH in the right ventricle was 6.97 and dropped to 6.82 during 10 minutes of global ischemia. During reperfusion with pH 7.6 blood cardioplegia the pH rose to 7.33. The pH tracing from Dog28I is included as Figure 5. Here the pH starts at 6.84, dropping to 6.74 as a result of ischemia and rising to pH 7.61 during reperfusion. Because of the rapid rise and fall in pH during this experiment, spectral and pH data were collected every 30 seconds.

4.2 Rabbit Experiments

A full wavelength calibration model was calculated for each rabbit experiment where reliable absorption spectra were recorded (R3J to R14J). The results of each of these calibrations is summarized in Table II. For the Ocean Optics System the complete range of acquired spectral data was used in the model. It was possible to collect data on the NIRSystems over the range of 400-2500 nm; however, the usable data was limited by the appearance of strong water absorbance bands on some of the spectra at (1440 nm and 1930 nm). Figure 6 shows a typical set of NIR reflection spectra for a rabbit muscle flap covered with skin for rabbit R9J. The number of pH data points used for the model averaged 11 for models where only arterial ligation was measured and 34 where both ischemia and reperfusion was studied. The optimum number of factors for the model was generally lower in unidirectional models than in models which utilized increasing and decreasing pH. Values for R^2 and RMSD, the parameters which describe the predictability of the model, were excellent, averaging 0.934 and 0.039 pH units, respectively, for all experiments. Figure 7 is a plot of actual versus predicted pH for rabbit R11J over the range 7.29-6.40 pH units. The R^2 value of 0.986 describes how well those points fit the perfect line of one, and the RMSD of 0.023 pH units is a prediction of the error that can be expected from the model.

The Ocean Optics and NIRSystems spectrometers were compared in terms of the model parameters R^2 and RMSD. The mean R^2 for data collected on the Ocean Optics spectrometer was 0.890 ± 0.072 , while the R^2 for the NIR Systems data was 0.960 ± 0.038 . Analysis of variance showed that the NIRSystems data was significantly better ($p=0.022$). RMSD values for the two systems: 0.047 ± 0.023 for the Ocean Optics and 0.035 ± 0.026 for the NIRSystems, were not significantly different ($p=0.372$) between the two spectrometers.

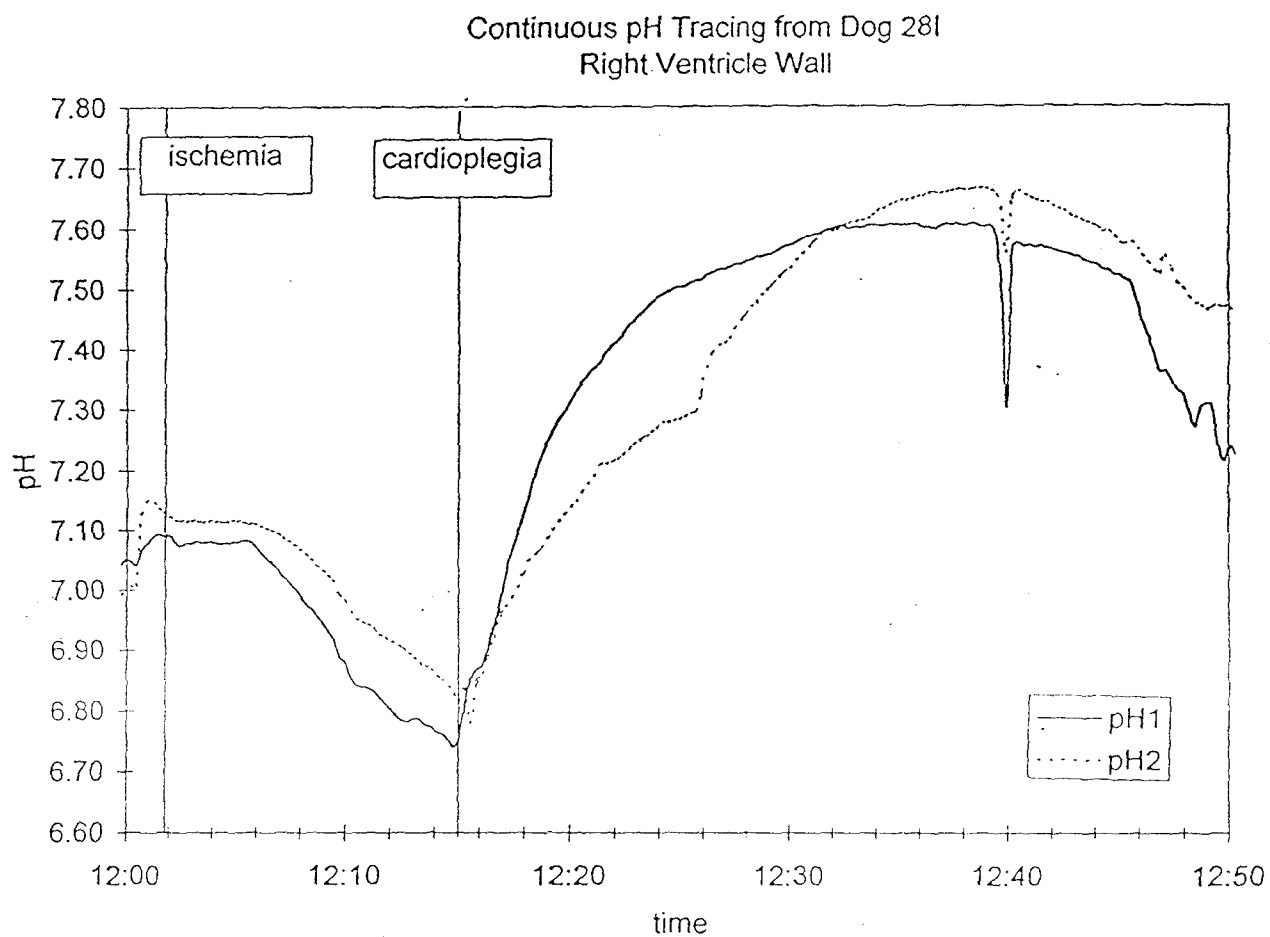


Figure 5. Continuous microelectrode pH traces for electrodes 1 and 2 in Dog 281, right heart ventricle wall

With Skin Flap, Decreasing pH

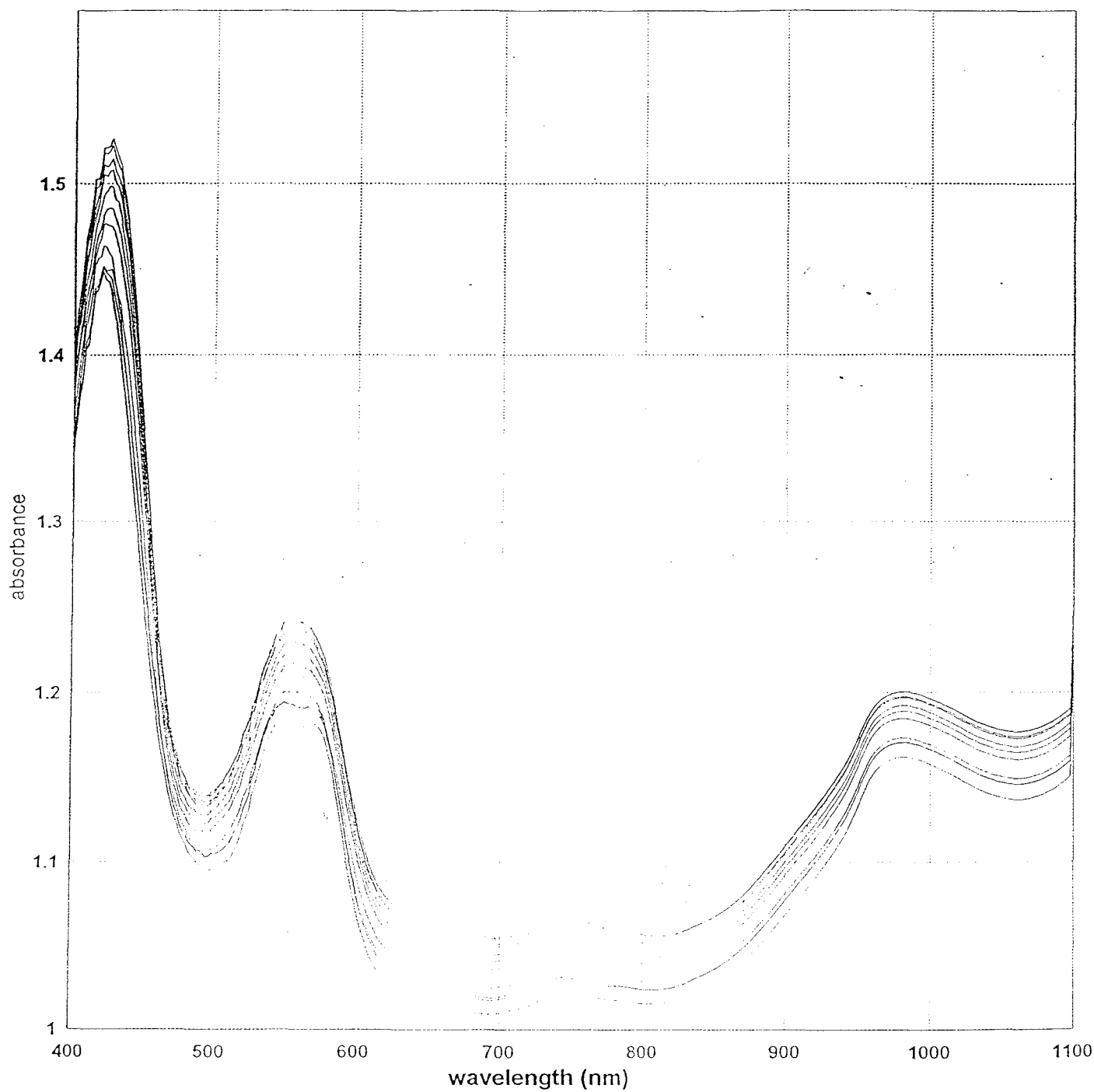


Figure 6. NIR reflection spectra of rabbit muscle flap covered with skin, measured with the NIR Systems spectrometer (60° angle probe), at different pH levels, for Rabbit 9J. This series of spectra were measured during decreasing pH after ligation.

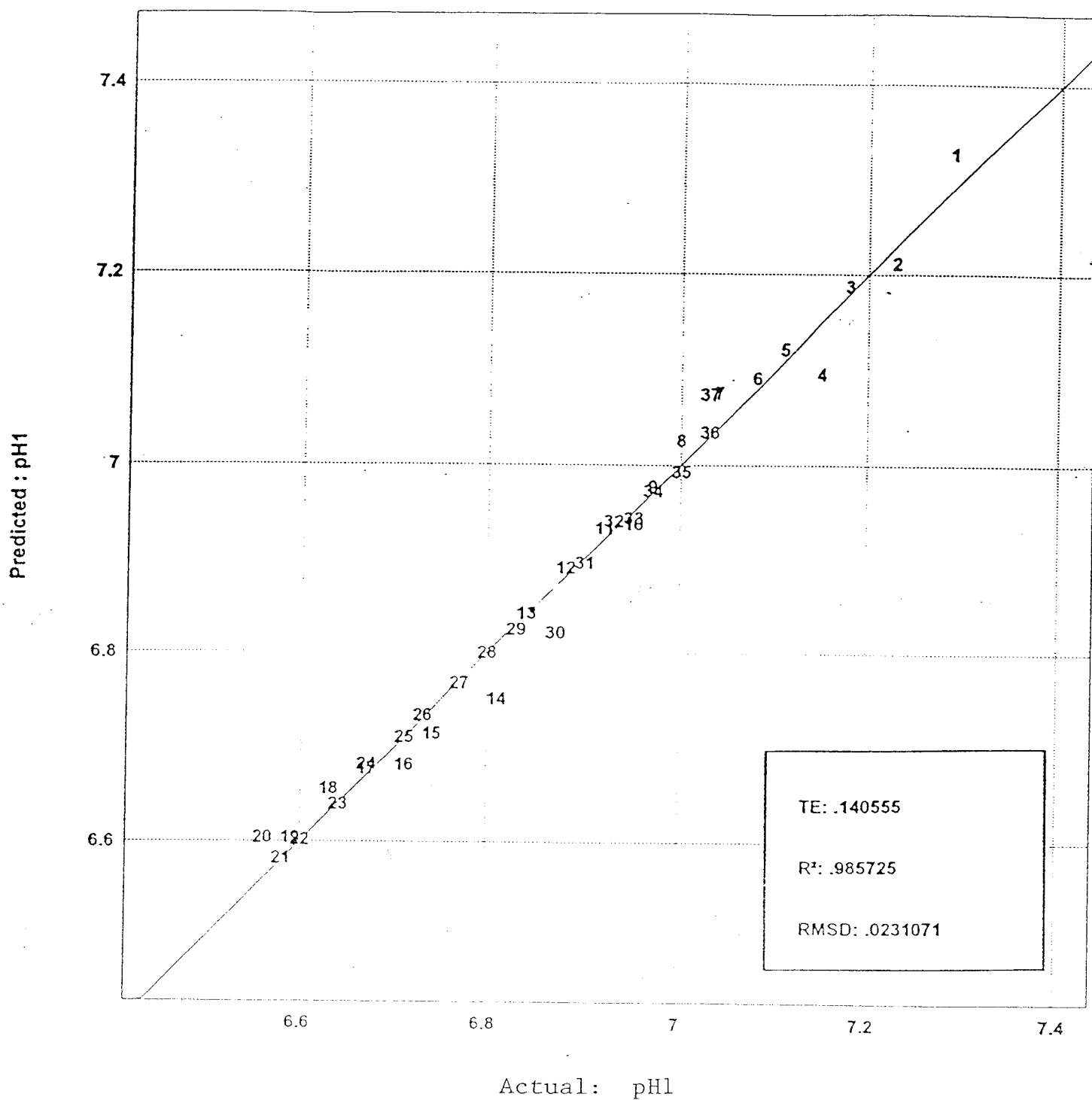


Figure 7. Partial least squares calibration verification plot of actual vs. predicted pH (from NIR spectra) for Rabbit 11J with bare muscle covered with skin flap including decreasing and increasing pH points

Table II. Model Statistics Derived from Rabbit Experiments. Best PLS Multivariate Calibration Model
Full Wavelength Range

experiment number	spectrometer	optical probe	wavelength range (nm)	# data points	pH range	no. of factors	R ²	RMSD
R3J left	Ocean Optics	angled	500-1000	12	6.81-6.50	1	0.902	0.033
R4J right	Ocean Optics	angled	500-1000	14	7.17-6.72	2	0.869	0.056
R4J, right, skin	Ocean Optics	angled	500-1000	11	7.14-6.91	2	0.916	0.023
R5J right	Ocean Optics	collinear	500-1000	14	7.36-6.76	6	0.955	0.047
R6J left	Ocean Optics	collinear	500-1000	8	7.11-7.45	3	0.942	0.033
R7J right	NIRSystems	angled (30°)	1100-1400	29	7.22-6.72-7.46	6	0.866	0.093
R8J left	Ocean Optics	collinear	500-1000	9	7.04-6.55	2	0.757	0.087
R9J right	NIRSystems	angled (60°)	400-1250	36	7.64-6.98-7.64	10	0.978	0.033
R9J, right, skin	NIRSystems	angled (60°)	400-2000	12	7.64-7.13	2	0.957	0.068
R10J right	NIRSystems	angled (60°)	400-1375	37	7.20-6.65-7.22	7	0.970	0.033
R10J right, skin	NIRSystems	angled (60°)	400-1900	27	7.22-6.90-7.25	6	0.923	0.030
R11J right, skin	NIRSystems	angled (60°)	400-1380	37	7.29-6.56-7.03	6	0.986	0.023
R12J right, skin	NIRSystems	angled (60°)	400-1350	26	7.21-7.02-7.35	3	0.978	0.015
R13J right, skin	NIRSystems	angled (60°)	400-1350	44	7.35-6.77-7.23	9	0.979	0.024
R14J right, skin	NIRSystems	angled (60°)	400-2000	35	6.95-6.74-7.18	5	0.993	0.011
R14J left, skin	NIRSystems	angled (60°)	400-1400	33	6.75-6.42-6.75	7	0.974	0.016

The wavelength region 700-1100 nm was chosen as the optimal wavelength region to prevent interference from water absorption and to maximize depth penetration of the sensor. Water has only low absorbance below 1300 nm, and experiments examining the depth penetration of near-infrared light in meat samples showed the greatest depth penetration between 700 and 1100 nm. Comparison of the model parameters R^2 and RMSD between full wavelength models and models derived from the 700-1100 nm region are shown in Table III for rabbits R10J - R14J, data collected with a skin flap in place. The mean R^2 for the 700-1100 nm range, 0.984 ± 0.011 , was greater than that for the full wavelength range model: 0.972 ± 0.025 ; however, for these six experiments there was no statistically significant difference. Similarly RMSD for the 700-1100 nm range model was 0.016 ± 0.006 pH units, compared to 0.020 ± 0.007 pH units, a smaller prediction error for the 700-1100 nm model, but not statistically significant.

The wavelength region 700-1100 nm was used to measure the actual prediction error for the determined models. Ten percent of the samples were removed before determining the model and the reduced set model was used to calculate the pH of remaining samples from the spectra alone. Table IV shows the average prediction error for 6 different experiments on 5 animals. **For these 6 studies on individual animals the average error in non-invasively measuring pH with 200 wavelengths between 700 - 1100 nm is $-0.006 \pm .009$ pH units.**

In one experiment the effect of changing probe height above the sample was studied. As the pH was lowered by ligation, 17 of the data points were collected from a probe that was positioned 2.5 mm above the muscle surface, 9 of the points were collected at 4.5 mm above the surface and 6 of the points were collected at 1.5 mm from the surface. The first model was derived using only the 17 points collected from the 2.5 mm position. Using that model to predict the points collected at the other heights resulted in an error of 0.151 pH units. A second model was derived using all the points except one point at each height. That model was used to predict the pH of the left out spectra. That model resulted in an average error of -0.006 pH units for the 3 points. This latter result indicates that calibration models can be developed that are not sensitive to the probe height.

4.3 Dog Experiments

Models derived from pH and spectral data collected from 2 dogs during open heart surgery are presented in Table V. The predicted versus actual pH plot for Dog 28I is presented in Figure 8 where pH varied between 6.74-7.61 and spectral data was collected from 700-1100 nm. The model parameters (R^2 : 0.979, RMSD: 0.046 pH units) are quite good for the dog, despite the fact that the probe height over the heart kept changing due to the heart beating during part of the ischemic period and reperfusion with a large volume of blood cardioplegia which caused the heart to bulge. Again, these results show that variation in the probe height on the order of 2 mm does not lead to significant measurement errors.

It is significant to note that the spectra in these two experiments were acquired with 16 scans with a collection time of only about 15 sec. The resulting signal/noise in the spectra was still excellent.

Table III. Comparison of Model Statistics for Two Different Wavelength Regions

experiment number	full range R^2	700-1100 nm R^2	full range RMDS	700-1100 nm RMDS
R10J right, skin	0.923	0.988	0.030	0.011
R11J right, skin	0.986	0.996	0.023	0.014
R12J right, skin	0.978	0.984	0.015	0.013
R13J right, skin	0.979	0.972	0.024	0.026
R14J right, skin	0.993	0.994	0.011	0.010
R14J left, skin	0.974	0.968	0.016	0.019

Table IV. Predicted pH for Deep Muscle Tissue covered with a Skin Flap: 700-1100 nm

experiment number	pH range	number of points predicted	average error of prediction (actual - predicted pH)
R10J	6.98-7.25	3	-0.003 pH units
R11J	6.53-7.41	4	-0.012 pH units
R12J	7.02-7.35	3	-0.011 pH units
R13J	6.77-7.33	4	+0.011 pH units
R14JR	6.74-7.16	3	-0.009 pH units
R14JL	6.41-6.75	3	-0.014 pH units

Table V. Model Statistics Derived from Canine Experiments. Best PLS Multivariate Calibration Model
Wavelength Range 700-1100 nm

experiment number	spectrometer	optical probe	wavelength range (nm)	# data points	pH range	no. of factors	R^2	RMDS
D27I	NIRSystems	angled (60°)	700-1100	16	6.97-6.82-7.33	8	0.979	0.028
D28I	NIRSystems	angled (60°)	700-1100	32	6.84-6.74-7.61	9	0.979	0.046

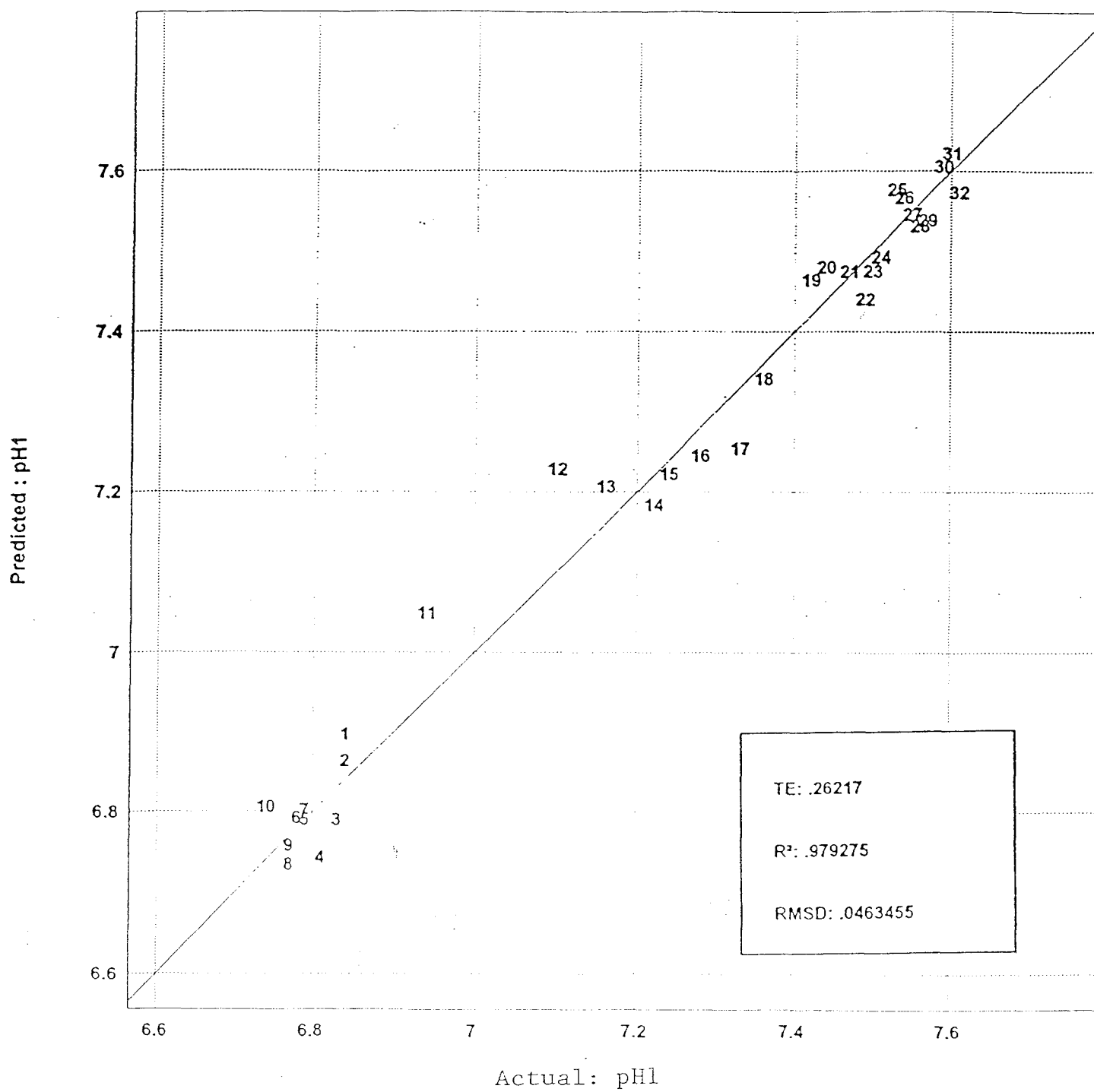


Figure 8. Partial least squares calibration verification plot of actual vs. predicted pH (from NIR spectra) for Dog 28I, right ventricle on cardiopulmonary bypass including decreasing and increasing pH points

4.4 Myoglobin as a Model Compound for the NIR Spectral Determination of pH in Muscle Tissue

An experiment was conducted to investigate horse heart myoglobin as a model compound for the sensitivity of NIR absorption spectra of muscle tissue to pH. Myoglobin is a major component of muscle tissue, and the variation of its spectral features with pH should be similar to that of many other compounds present in muscle tissue. As described above in the experimental section, myoglobin was dissolved in pH buffer solutions for 11 different pH values, evenly spaced, in the 6.3 - 7.3 pH range.

The NIR spectra and known pH data were analyzed with the same PLS multivariate calibration software used with the rabbit and dog experiment data. Figure 9 shows the set of NIR transmission spectra from this experiment. The spectra show one broad absorption band in the 700 - 1400 nm range. An actual vs. predicted pH PLS calibration plot is shown in Figure 10. The PLS analysis results show a R^2 value of 0.902, a RMSD error of 0.091 pH units and an average prediction error or bias of 0.08 pH units for 3 data points of pH 6.45, 7.20, and 7.20 predicted with a model developed from the remaining 20 data points. The results show agreement with the trends observed for pH vs. NIR spectral relations in the rabbit and dog experiments.

4.5 Analysis of NIR Spectra and pH Data to Determine Minimum Required Spectral Resolution Elements

An important question to answer for further development of the NIR reflection deep tissue pH monitor is determining the minimum number of resolution elements required in a NIR reflection spectrum to obtain accurate pH measurements with a precision in the range of 0.01 to 0.05 pH units. Major reductions in the size and cost of the NIR pH monitor instrumentation could be achieved by the use of a set of light emitting diode light sources combined with a photodiode detector, in place of the higher resolution diffraction grating based spectrometers used in the Phase I effort.

To determine the minimum required spectral resolution, the NIR spectra and pH electrode data from two rabbit experiments were reanalyzed using an option in the PLS software package which permits spectrally deresolving the spectra. As an example of this desresolution process, the software can average the 276 data points in the NIR spectra in the 700 - 1250 nm range in groups of 28 points to produce a deresolved spectrum with just 10 data points representing averages for successive 28 point regions. These deresolved NIR spectra were produced from the data from two rabbit experiments and then analyzed with the PLS software to produce a calibration model. Figure 11 shows an example of a NIR reflection spectrum from a rabbit experiment in normal and deresolved form. PLS actual vs. predicted pH calibration plots are given in Figure 12 using the normal resolution of the NIR Systems spectrometer of 276 data points for the 700 - 1250 nm region and for 10 averaged data points. The resulting R^2 and RMSD error values for the PLS calibration model actually improved slightly from 0.995 and

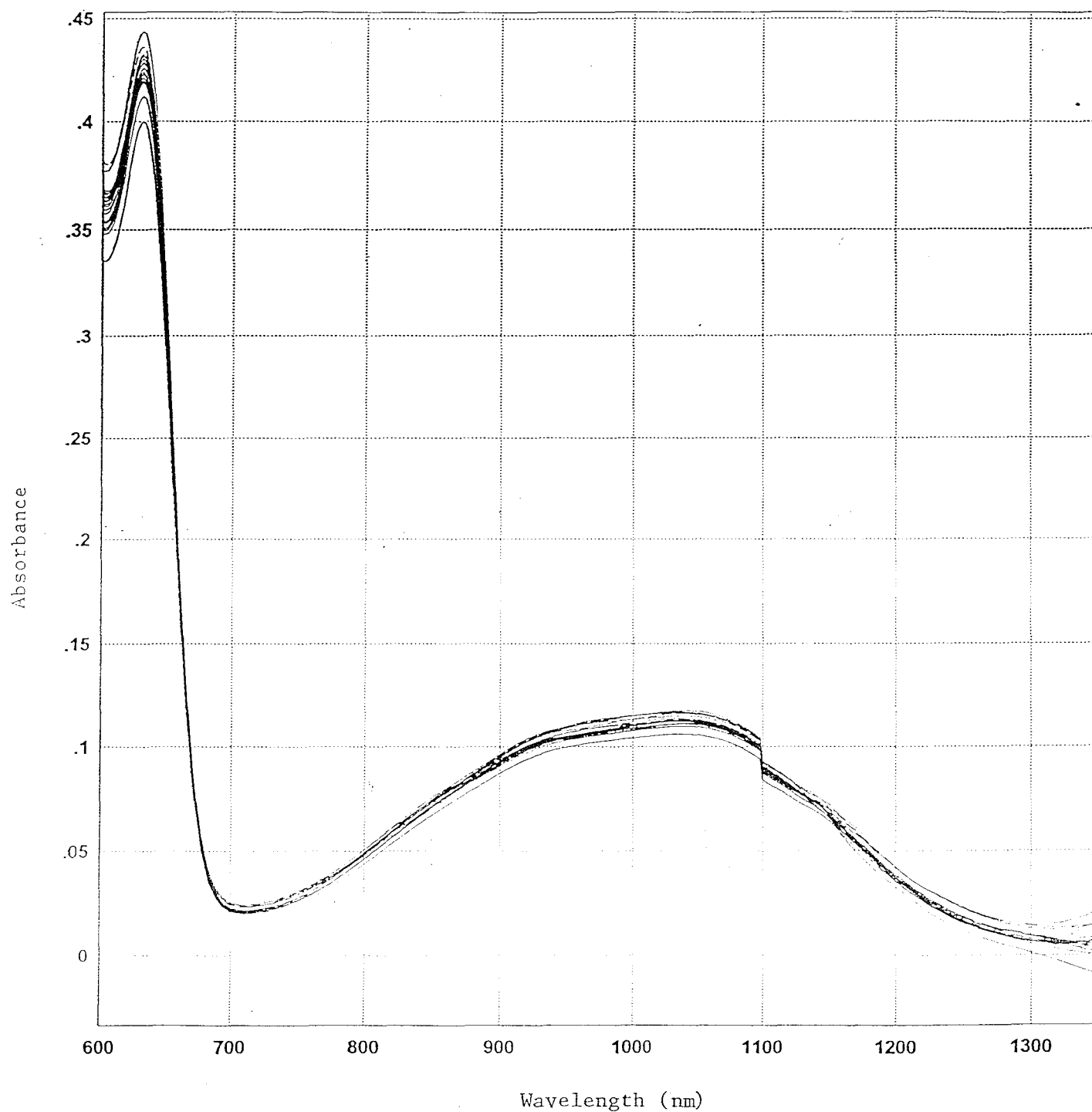


Figure 9. Transmission spectra for 23 myoglobin samples dissolved in different pH buffers in the range of 7.3-6.3 pH units

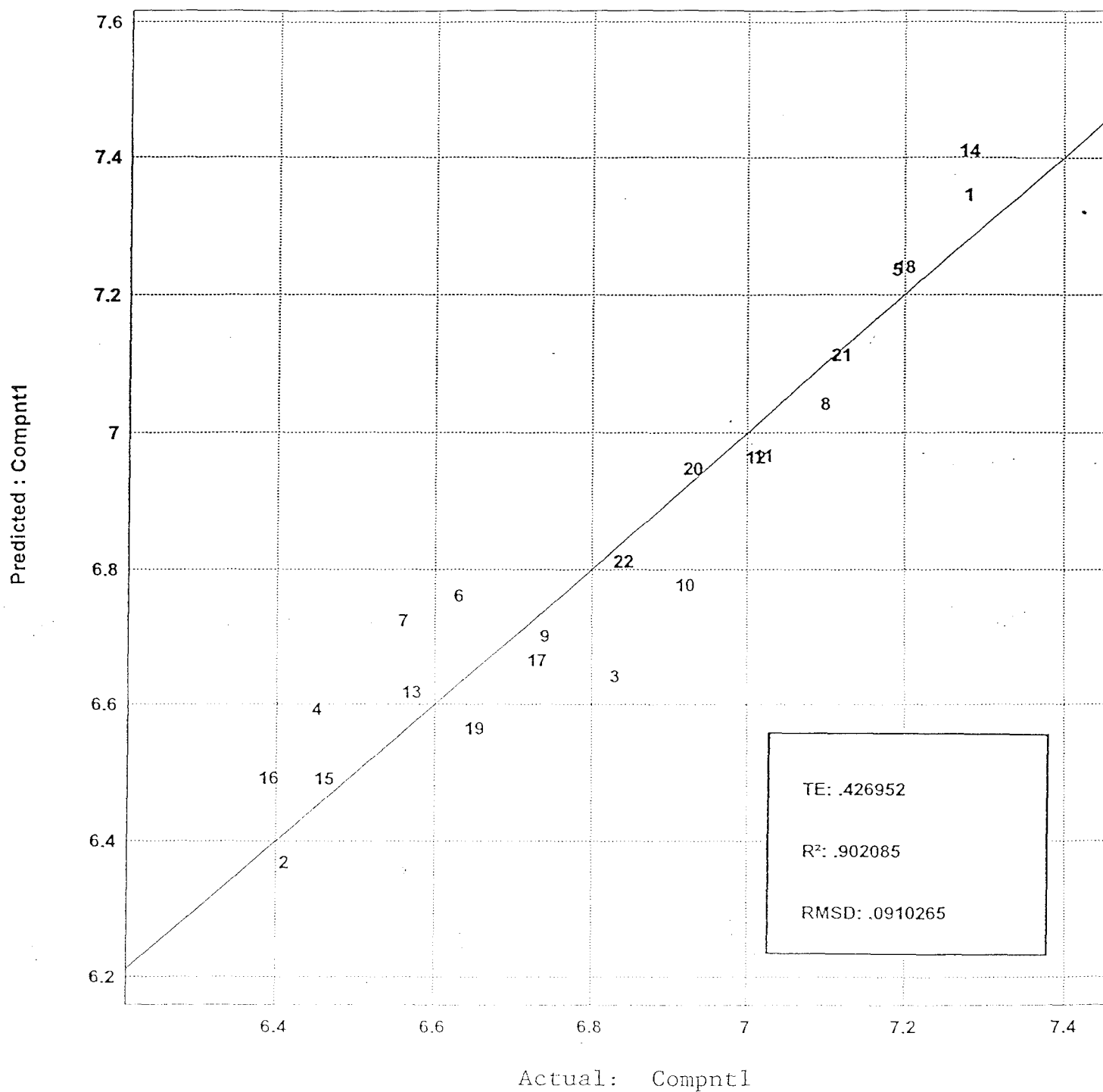


Figure 10. Partial least squares calibration plot of actual vs. predicted pH (from NIR spectra) for myoglobin dissolved in pH buffer solutions

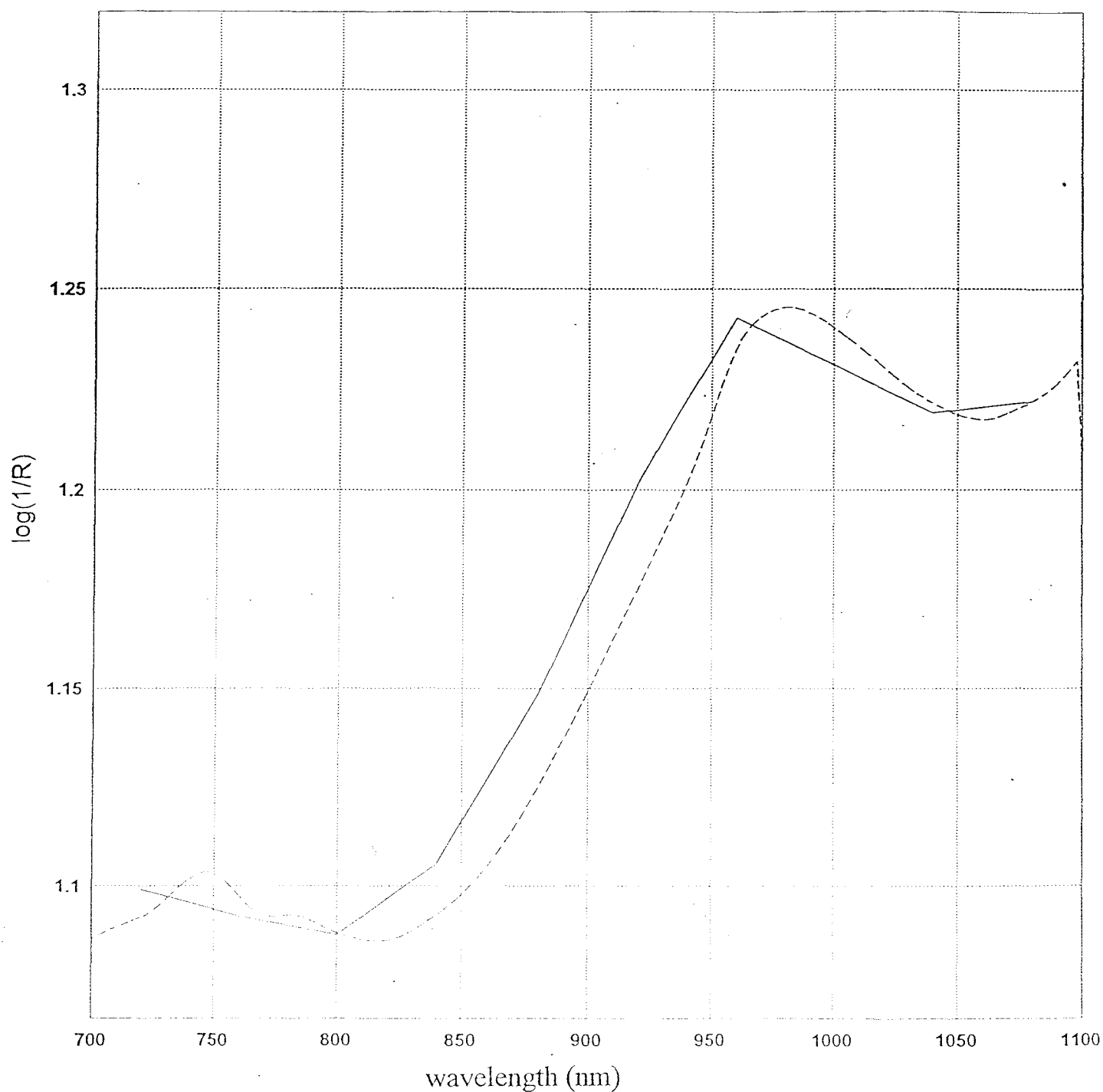
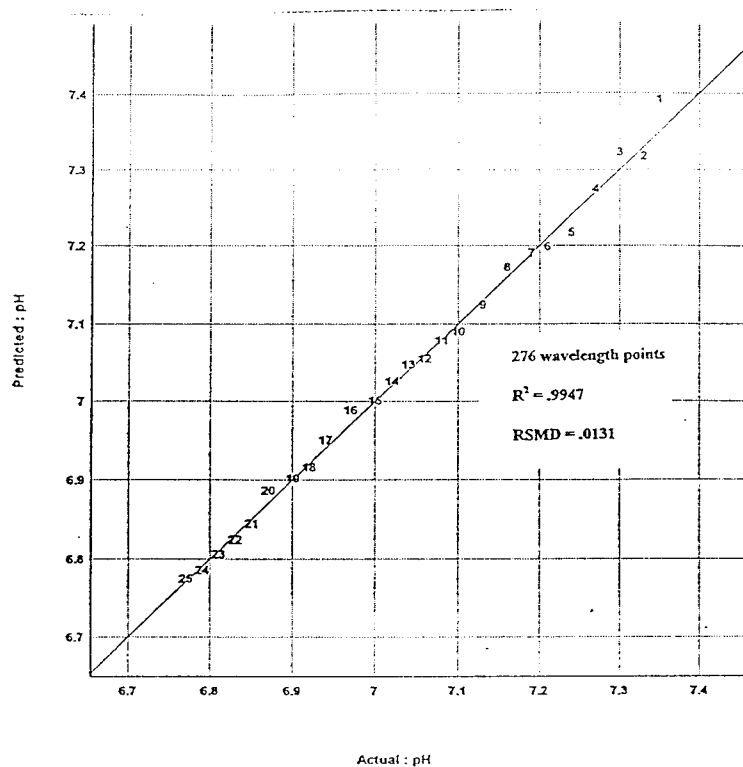


Figure 11. NIR reflection spectrum of rabbit muscle tissue with normal resolution of 201 wavelength points in 700-1100 nm range (dashed spectrum), and deresolved to 11 wavelength points (solid curve)

a)



b)

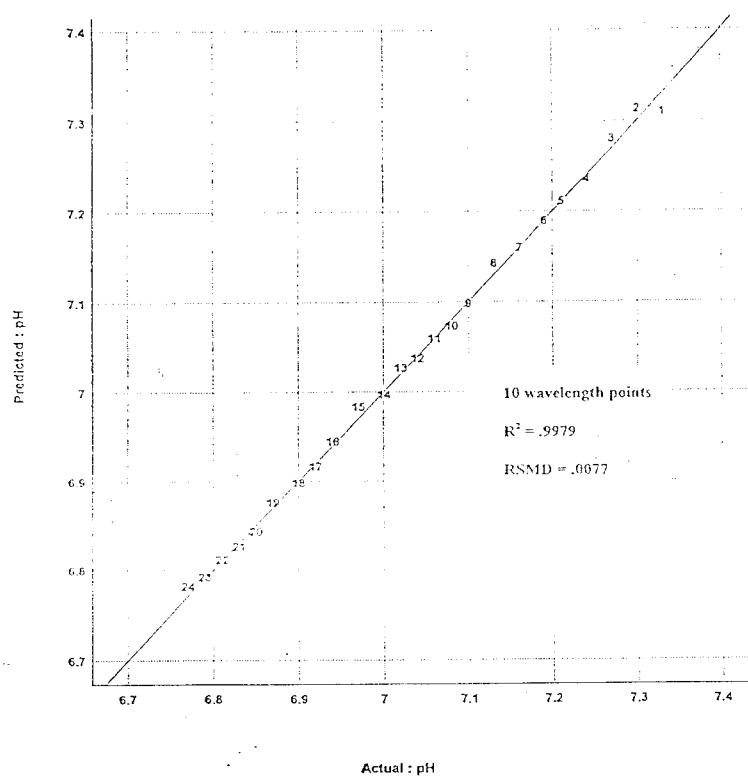


Figure 12. Partial least squares calibration verification plot of actual vs. predicted pH (from NIR spectra) for Rabbit 13J with (a) normal spectral resolution of 276 wavelength points in 700-1250 nm range, (b) deresolved spectra with Only 10 wavelength intervals in the 700-1250 nm range

0.013 to 0.997 and 0.008 for the deresolved spectra. A similar test was done with a second data set from another rabbit experiment in which the number of data points was reduced from 200 points for the 700 - 1100 nm region to 11 averaged points. In this second test additional calibration model validation was done by removing 3 spectra from the original set of 27 and predicting the pH from these spectra with the PLS model developed from the remaining 24 spectra and corresponding known micro-electrode pH values. The results for this latter deresolved data were very close to the original values with a very slight improvement in values from an R^2 and RMSD of 0.990 and 0.011 to 0.986 and 0.013. The deviation or bias of the 3 independently predicted pH values compared to the actual values from this latter data set increased slightly from -0.003 to -0.005 pH units but is still quite acceptable. The results clearly demonstrate that the optimal 700 - 1250 nm region can be adequately measured with only 10 or 11 wavelength points representing the average reflectance information in each of these 10 or 11 wavelength bands.

4.6 Experiments to Determine the Depth Penetration of the NIR Reflection Technique for Tissue pH Measurement

Several experiments were conducted to determine the depth penetration as a function of wavelength for the reflected NIR light used to probe the tissue pH in this program. As previously described in Section 3.6, a fixture was constructed to permit an aluminum mirror to slide underneath a flank steak sample which is supported to leave a 0.5" x 0.75" unobstructed area between the mirror and the sample through which transmitted and reflected NIR light can pass.

The results of one of these experiments produced the NIR spectra shown in Figure 13 which gives reflection spectra for a 7 mm thick flank steak sample with and without the mirror underneath the sample. This composite spectrum shows a significant increase in reflectance, shown as a decrease in $\log(1/R)$ (where R is fractional reflectance), when the mirror is present. These spectra show that the wavelength region for maximum depth penetration is in the 750 - 1125 nm range. Within this wavelength range, the results show a measurable amount of light passing through the 7 mm sample thickness, bouncing off the mirror and then passing through the sample a second time before reaching the receiving fiber bundle and going to the spectrometer detector. An absorbance change of about 0.015 - 0.02 absorbance units, on a baseline absorbance of about 1.5, is produced by the mirror in the 750 - 1125 nm range, which indicates that about 10% of the light reaching the detector, penetrates down to 7 mm.

5.0 DISCUSSION

It has been demonstrated that deep muscle pH can be reliably measured using non-invasive techniques. By analyzing the reflection of near-infrared light using multivariate calibration techniques, measurement of changes in pH in skin covered rabbit muscle and in the canine heart on cardiopulmonary bypass during both ischemia and reperfusion was demonstrated.

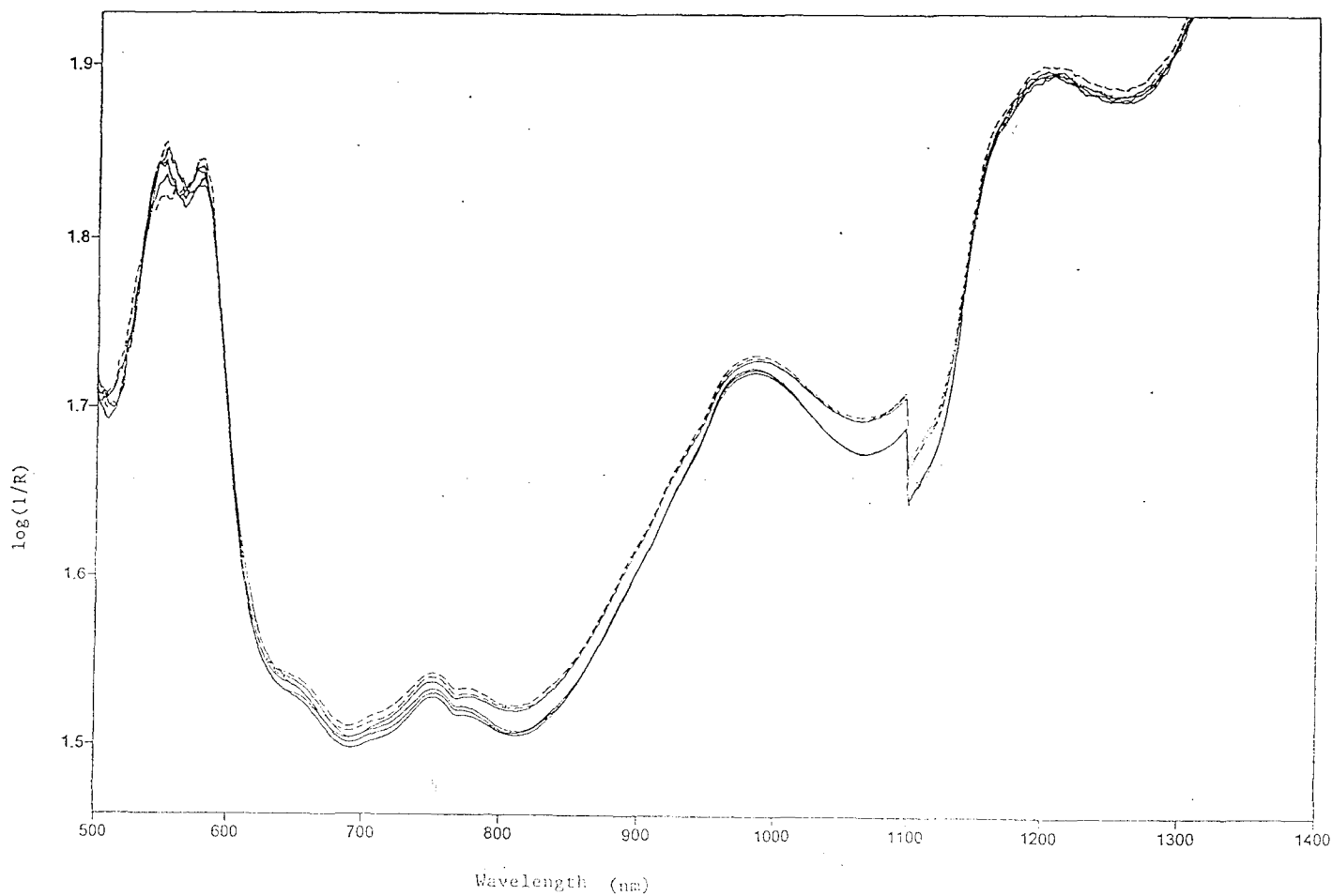


Figure 13. NIR reflection spectra of a 7 mm thick flank steak sample, showing 3 spectra measured with an aluminum mirror behind the sample (solid curves), and 3 spectra without a mirror behind the sample (dashed curves). The mirror increases the reflected signal due to light passing through the sample Thickness in the 700-1125 nm wavelength range

While the requirements of the program demand rapid detection of falling pH, data is included on increasing pH values to demonstrate that this technique is measuring changes in pH and not some other parameter. There is only one reference in the literature on using near-infrared spectra to measure pH (16), and this was demonstrated on the bench, in solution, over a different wavelength region with large errors (0.3 pH units). For this reason it was deemed important to validate this current research method by incorporating at least two independent measurements of spectral data at the same or near same pH. In the early experiments the pH was reduced by ligating the vessel, and measurements taken at regular time intervals. To assure that changes in spectra were not the result of other in-vivo changes that might be occurring at the same time, in subsequent experiments, pH was decreased by ligation and then increased by reperfusion of the same muscle. The achievement of excellent model parameters with pH values during both ischemia and reperfusion is proof that the actual measurements were of pH and not such factors as the muscle drying out, which might also be directly correlated with time. Additionally, the data collection technique was modified to record spectra every 0.02 pH units, no matter how long it took to achieve that change. This further validated this technique as a true measure of pH.

This experimental technique was repeated in 6 experiments on 5 different animals (R10J-R14J) collecting near-infrared light at 200 wavelengths between 700-1100 nm on muscle which was covered by shaved rabbit skin. This data, shown in Table IV, demonstrates that the method can be reliably performed on different subjects with accuracy which is significantly better than 0.05 pH units. While the calibration models for each of the rabbit subjects is different, future work will involve the development of a generalized model which would be applicable to all subjects. Polestar's early results on in-vivo subjects are comparable or superior to early results achieved by Robinson et. al. (11) who measured glucose levels in three diabetic patients. Their prediction errors were approximately 10% of the average blood glucose levels of their patients.

The demands of a body-worn sensor require it to operate despite changes in position relative to the skin surface. Though most of these experiments were carried out at constant height relative to the skin surface, it was demonstrated in a separate experiment that small changes in sensor position can be compensated for as long as they are anticipated in developing the calibration equations. In general, the multivariate calibration methodology is robust enough to incorporate most variations encountered during the use of the sensor, as long as they are anticipated in advance.

Analysis of the data from two of the rabbit experiments has demonstrated that a spectral resolution for the near-infrared reflection spectra which is much lower than that used in the Phase I effort can be successfully employed in measuring pH. Re-analysis of the rabbit data showed that when the spectra were deresolved by mathematical averaging to only 10 resolution intervals for the 700 - 1250 nm range (from 276), or 11 intervals for the 700 - 1100 nm range, that the accuracy of the optically detected pH accuracy was not impaired. This result is very significant in that it shows that a highly simplified and miniaturized spectrometer system based on 10 or 11 light emitting diode light sources together with two photodiode detectors could be used to monitor tissue pH. Such a simplified spectrometer system is discussed in more detail below in the section on a conceptual design for the next version of the near-infrared pH monitor.

Significant penetration of the near-infrared reflectance measurement in the 700 - 1100 nm wavelength region has been measured down to a depth of 7 mm with 10% light return to the detector in an experiment with a piece of flank steak. This result is consistent with near-infrared transmission measurements of meat protein and fat content reported in the literature (10) for 15 mm thick samples in a similar wavelength region. The transmission measurement permits greater sample thickness since the light only makes a single pass through the sample thickness.

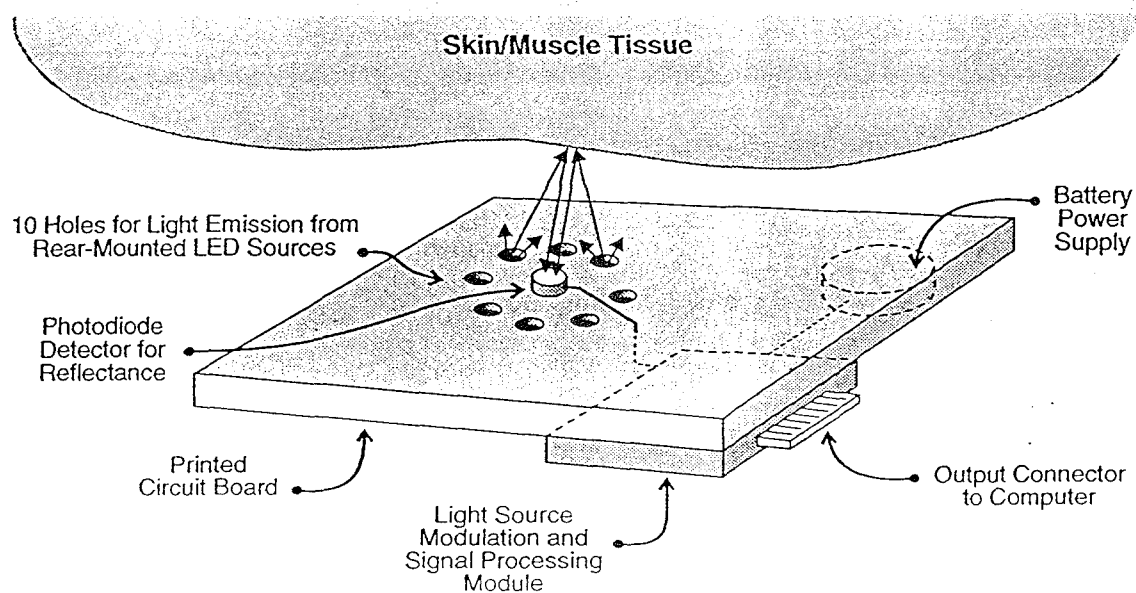
A experiment was performed with myoglobin to help gain insight into the detailed mechanism for the pH sensitivity of the near-infrared spectra of muscle tissue. Near-infrared transmission spectra for a series of myoglobin solutions in pH buffer solutions prepared to evenly span the 7.3 - 6.3 pH range, were analyzed together with the known pH values using PLS regression analysis. The results exhibited a similar correlation of subtle changes in the spectra with pH as found for the rabbit muscle tissue. The pH dependence of muscle tissue is likely to be a summation of pH induced changes in several broad and overlapping spectral bands due to myoglobin and other pigments present in muscle tissue such as cytochromes, flavoproteins, pyridine nucleotides, hemoglobin, and melanin, as well as the contribution of a minor water band.

6.0 CONCEPTUAL DESIGN FOR PROTOTYPE MINIATURE NEAR-INFRARED DEEP TISSUE pH MONITOR

A conceptual design for a miniaturized NIR reflection spectrometer system for non-invasive deep tissue pH monitoring has been developed for use in applications requiring a portable, compact, lightweight, and low cost instrument. This pH monitoring system is designed for field diagnosis of hemorrhage induced shock in combat casualties or for other medical applications such as diagnosis of trauma victims in hospital emergency rooms, ambulances and evacuation helicopters.

In this design the NIR spectrometer is based on 10 light emitting diode (LED) light sources at different wavelengths which reflect off of the target tissue area and are detected with a photodiode detector. The design for this spectrometer system is shown in the diagram in Figure 14. The LED sources will be selected to cover the 700 - 1100 nm wavelength range at 10 even intervals with typical LED emission bandwidths of about 60 nm. As described above in Section 4.5, it was determined from the NIR spectral data obtained for the Phase I effort rabbit experiments that a reflection spectrum with 10 resolution elements would permit the same pH measurement precision and accuracy as the 201 element spectra measured in the Phase I work for the same wavelength range. In the LED spectrometer, the LED sources will be pulsed in sequence with programmed modulation of the power supply voltage and then the corresponding reflected light signals will be detected with a photodiode detector. The signal from the reflection photodiode detector will be separated into the 10 individual LED components with a phase sensitive amplifier system synchronized to the LED modulation source, and will output to a computer for data analysis. The final signal sent to the computer will be normalized for LED source intensity variations by the signal from a reference photodiode on the back side of the spectrometer board which receives direct light from the LEDs. A reflector over the LEDs on

TOP PERSPECTIVE VIEW



SIDE VIEW

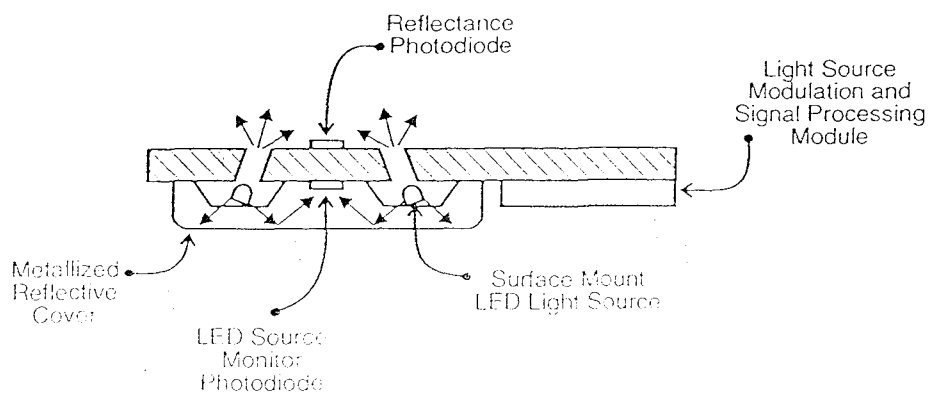


Figure 14. Conceptual design for compact deep tissue pH sensor. Sensor measures reflected light from 10 light emitting diode (LED) light sources with 10 different emission wavelengths. Scale is life size.

the back side of the spectrometer card is used to increase the direct LED signal to the reference detector. The LED pulsed power source and the signal processing electronics are contained in a single electronics module on the back side of the system. This spectrometer card will be held within about 1 mm of the target tissue surface with an appropriate plastic spacer. The data analysis will be performed using PLS or other multivariate analysis methods on the computer interfaced with the spectrometer card output.

This design is much simpler, lower cost, and more amenable to miniaturization than the diffraction grating based dispersive spectrometers employed in the Phase I effort. This type of LED spectrometer could be further miniaturized to be mounted within a single integrated circuit package.

7.0 RECOMMENDATIONS FOR CONTINUED WORK

Given the overall program goal of developing miniature, body-worn sensors designed to fuse data with sensors monitoring other physical and chemical parameters, Polestar Technologies recommends that efforts in Phase II focus on the further characterization and optimization of this non-invasive technique. These efforts will include development of a breadboard NIR pH monitor, characterization and testing of the technique with animal subjects, development of a universal calibration model predicting pH from NIR reflection spectra for different animal subjects, and design and fabrication of a miniaturized prototype LED pH monitor for testing and evaluation by the Army, as well as civilian trauma units. Additionally, work needs to be done to develop methods of extending animal calibration procedures to human use.

8.0 CONCLUSIONS

The Phase I effort has successfully demonstrated that tissue pH can be measured using near-infrared reflection spectroscopy coupled with partial least squares analysis (PLS) in skin covered rabbit muscle and a canine heart on cardiopulmonary bypass. In six separate determinations of deep tissue pH in the rabbit teres major muscle, the derived model was capable of measuring pH from collected spectra to an average accuracy of -0.006 ± 0.009 pH units.

Experiments were conducted using two different spectrometers and a variety of fiber optic probes. Models from these configurations were compared using statistics derived from the PLS cross-validation analysis. By comparing R^2 and RMDS values from these models, we were able to determine that the NIR Systems spectrometer provided superior data collection, most likely because of its larger diameter source and fiber probes and a more stable detection. Using similar techniques, we were able to demonstrate that the wavelength region 700-1100 nm provided the most accurate models. By collecting data on both the canine heart and the rabbit muscle we have shown the potential of this technique for both military and civilian applications. The most

important characteristics of the prototype pH monitoring system developed in the Phase I effort are summarized below:

- a pH accuracy of 0.01 pH units in muscle tissue covered with skin
- significant measurement penetration down to a depth of 7 mm
- insensitivity to probe height from skin/muscle surface
- a measurement time of 15 sec.
- successful performance for monitoring pH in the teres major muscle in rabbit subjects and heart muscle pH in dog subjects
- reproducible partial least squares calibration model results with R^2 coefficient better than 0.98 and route mean square deviation errors less than 0.02 pH units for 5 rabbit experiments
- an optimal wavelength range of 700 - 1100 nm
- a required spectral resolution of 10 or fewer resolution elements for the 700 - 1100 nm range, demonstrating feasibility for a compact multi-wavelength light emitting diode based instrument

These results led to the development of a conceptual design for a dedicated portable near-infrared pH monitor system for diagnosis of combat casualties in the field. This portable system will be highly miniaturized and will employ a set of light emitting diodes combined with photodiode detectors to collect spectral reflection data in the optimal wavelength region for deep tissue pH measurement.

9.0 REFERENCES

1. Takano K, Yosii S, Hosaka S, Hashimoto R, Matsukawa T, Tada Y. Muscle pH/PCO₂ monitoring. *J Pediatr Surg* 1993;28(10):1376-9.
2. Warner KG, Durham-Smith G, Butler MD, Attinger CE, Upton J, Khuri SF. Comparative response on muscle and subcutaneous tissue pH during arterial and venous occlusion in musculocutaneous flaps. *Ann Plast Surg* 1989;22:108-16.
3. Dunn RM, Kaplan IB, Mancoll J, Terzis JK, Trengove-Jones G. Experimental and clinical use of pH monitoring of free tissue transfers. *Ann Plast Surg* 1993;31:539-45.
4. Khuri SF, Josa M, Marston W, Braunwald NS, Smith B, Tow D, VanCisin M, Barsamian EM. First report of intramyocardial pH in man. II. Assessment of adequacy of myocardial preservation. *J Thorac Cardiovasc Surg* 1983;86:667-78.
5. Stahl RF, Soller BR, Hsi C, BelleIsle J, Vander Salm TJ. Falling myocardial pH reflects ischemia during continuous warm retrograde cardioplegic arrest. *Ann Thorac Surg* 1994;58:1645-50.
6. Hampson NB, Piantadosi CA. Near-infrared monitoring of human skeletal muscle oxygenation during forearm ischemia. *J Appl Physiol* 1988;64(6):2449-57.
7. Wilson JR, Mancini DM, McCully K, Ferraro N, Lanoce V, Chance B. Non-invasive detection of skeletal muscle underperfusion with near-infrared spectroscopy in patients with heart failure. *Circulation* 1989;80:1668-74.
8. Reeves J. Influence of pH, Ionic Strength, and Physical State on the Near-Infrared Spectra of Model Compounds. *J. of AOAC Internat* 1994;77(4):814-20.
9. Drennen JK, Gebhart BD, Krammer EG, Lodder RA. Near-infrared spectrometric determination of hydrogen ion, glucose, and human serum albumin in a simulated biological matrix. *Spectroscopy* 1991;6(2):28-36.
10. Isaksson, T, Miller, C, and Naes, T. Nondestructive NIR and NIT Determination of Protein, Fat, and Water in Plastic-Wrapped, Homogenized Meat. *Appl. Spectrosc.* 1992;46:1685.
11. Lanza E. *J. Food Science*, 1983;48:471.
12. Geladi P, MacDougall D, and Martens H. Linearization and Scatter-Correction for Near-Infrared Reflectance Spectra of Meat. *Applied Spectroscopy*, 1985;39:491.

13. Hall JW, Pollard A. Near-infrared spectrophotometry: A new dimension in clinical chemistry. Clin Chem 1992;38/9:1623-31.
14. Haaland DM, Robinson MR, Koepp GW, Thomas EV, Eaton RP. Reagentless near-infrared determination of glucose in whole blood using multivariate calibration. Appl Spectrosc 1992;46(10):1575-8.
15. Ward KJ, Haaland DM, Robinson MR, Eaton RP. Post-prandial blood glucose determination by quantitative mid-infrared spectroscopy. Appl Spectrosc 1992;46(6):959-65.
16. Robinson MR, Eaton RP, Haaland DM, Koepp GW, Thomas EV, Stallard BR, Robinson PL. Non-invasive glucose monitoring in diabetic patients: A preliminary evaluation. Clin Chem 1992, 38(9):1618-22.
17. Carney JM, Landrum W, Mayes L, Zou Y, Lodder RA. Near-infrared spectrophotometric monitoring of stroke-related changes in the protein and lipid composition of whole gerbil brains. Anal Chem 1993;65:1305-13.
18. Martens H. and Naes T. Multivariate Calibration. Chichester: John Wiley and Sons, 1989.
19. Beebe K, and Kowalski B. An Introduction to Multivariate Calibration and Analysis. Analytical Chem 1987;59:1007A.
20. Khuri SF, Marston W, Josa M, Crowe W, Macera R, Zierler M, Lange R, Miller W. First report of intramyocardial pH in man: I. Methodology and initial results. Medical Instrumentation 1984;18, No.3:167-71.
21. Thomas EV. A primer on multivariate calibration. Anal Chem 1994;66(15):795A-804A.
22. Haaland DM, Thomas EV. Partial least-squares methods for spectral analyses. 1. Relation to other quantitative calibration methods and the extraction of qualitative information. Anal Chem 1988;60:1193-202.

Received 2/8/00



DEPARTMENT OF THE ARMY
US ARMY MEDICAL RESEARCH AND MATERIEL COMMAND
504 SCOTT STREET
FORT DETRICK, MARYLAND 21702-5012

REPLY TO
ATTENTION OF:

MCMR-RMI-S (70-1y)

21 Jan 00

MEMORANDUM FOR Administrator, Defense Technical Information
Center, ATTN: DTIC-OCA, 8725 John J. Kingman
Road, Fort Belvoir, VA 22060-6218

SUBJECT: Request Change in Distribution Statement

1. The U.S. Army Medical Research and Materiel Command has reexamined the need for the limitation assigned to technical reports written for the attached Awards. Request the limited distribution statements for Accession Document Numbers listed be changed to "Approved for public release; distribution unlimited." These reports should be released to the National Technical Information Service.

2. Point of contact for this request is Ms. Virginia Miller at DSN 343-7327 or by email at virginia.miller@det.amedd.army.mil.

FOR THE COMMANDER:

Encl
as

A handwritten signature in cursive script, reading "Phylis Rinehart", is positioned above the printed name and title.
PHYLIS M. RINEHART
Deputy Chief of Staff for
Information Management